2010

Exploration of non-chemically amplified resists based on dissolution inhibitors for 193 nm lithography

Burak Baylav

Exploration of Non-Chemically Amplified Resists Based on Dissolution Inhibitors for 193 nm Lithography

By

Burak Baylav

A Thesis Submitted

in Partial Fulfillment

of the Requirements for the Degree of

Master of Science

in

Microelectronic Engineering

Approved by:

Prof. _____
Dr. Bruce W. Smith (Thesis Advisor)

Prof. _____
Dr. Thomas W. Smith (Committee Member)

Prof. _____
Prof. Dale Ewbank (Committee Member)

Dr. Paul Zimmerman (External Collaborator)

MICROELECTRONIC ENGINEERING PROGRAM
COLLEGE OF ENGINEERING
ROCHESTER INSTITUTE OF TECHNOLOGY
ROCHESTER, NEW YORK
JANUARY, 2010

Exploration of Non-Chemically Amplified Resists Based on Dissolution Inhibitors for 193 nm Lithography

By

Burak Baylav

_____ _____

Burak Baylav January, 2010

ABSTRACT

Research described in this work includes exploration of new resist systems that can be used for 193 nm lithography. Most of the conventional 193 nm resists rely on chemical amplification in which a small amount of photogenerated acid can catalyze many reactions. Even though the sensitivity is improved drastically with such a mechanism, the printed profiles are known to be suffering from line edge roughness (LER) and image blurring. Furthermore, the resolution is limited by the diffusion length of the generated acid. For sub-32 nm technology nodes, specified LER criterion cannot be satisfied by utilizing chemically amplified resists (CAR). However, improvements in laser power and lens materials enable relaxation in high sensitivity requirement for the resist materials. When low sensitive photomaterials are acceptable, chemical amplification in the resists can be reduced or can even be completely eliminated. In this research, reasons behind the need of using non-chemically amplified resists is explained and some possible solutions are explored. At the end, a two component resist system that utilizes nitrobenzyl cholate as dissolution inhibitor and poly norbornene hexafluoro alcohol as the base resin is shown to achieve dense line/space patterns at 150 nm, 120 nm and 90 nm half pitches.

TABLE OF CONTENTS

LIST OF TABLES

LIST OF FIGURES

Acknowledgments

I would like to acknowledge those people who helped me to complete this research. I am grateful to my academic advisor, Dr. Bruce W. Smith, for his continuous encouragement throughout this project. I would like to thank him for believing in the quality of my work and to have me a part of his research team. I have always felt honored to be in the same group with such brilliant minds.

I would like to thank my coworkers, Meng Zhao, Ran Yin, Darren Smith, Peng Xie and Neal Lafferty, for their valuable discussions and sharing the load of my work at hard times. I would like extend my sincere gratitude to Dr. Thomas W. Smith, Prof. Dale Ewbank and Dr. Paul Zimmerman for their guidance and support.

Also, I would like to acknowledge AZ Chemicals and Promerus LLC (Brecksville OH), particularly Dr. Ralph Dammel and Dr. Larry F. Rhodes, for generously donating some of the materials used in the experiments of this research.

Finally, I am so grateful for having such a wonderful mother and a brother who have been and will always be there for me.

Chapter 1

Introduction and Motivation

1.1 Chemical Amplification in Resists

The resist requirements for sub-32 nm are listed in ITRS (2007 Edition) for both near term (2007-2015) and long term (2016-2022) years. In 2013, the DRAM ½ pitch is given as 32 nm and resist thickness should be less than 100 nm to ensure low aspect ratio, thus avoiding pattern collapse problem. For the same year, ½ pitch for flash is 25.3 nm, and MPU gate length in resist is 21 nm [1]. Furthermore, following 2013, line width roughness (LWR) is specified to be less than 1.7 nm (3σ). This is unachievable for current chemically amplified resist (CAR) systems. The desired LWR falls below 1 nm for technology nodes introduced after 2019[1].

The reciprocal relationship between resolution and resist sensitivity is another drawback for chemically amplified resist systems. The mechanics of acid assisted chemical reactions during post exposure bake and the diffusion of generated acid are responsible for this trade-off. If, through improvements in laser power and lens elements, resist sensitivity is no longer specified as sub-50 mJ/cm^2, chemical amplification can be reduced or even be eliminated completely to enable better resolution and lower line edge roughness (LER).

The inherent limitations of CAR systems have been explored by many researchers starting from 248 nm resists[2]. The resolution of poly methyl methacrylate (PMMA) resist has shown to be superior to contemporary CARs. The former can resolve images below 20 nm; but the latter is not able to achieve good resolution below 30-35 nm even when the presented aerial image modulation is near unity[3]. The thermally driven acid diffusion in CAR has a different nature than main chain scissioning type resists (e.g. PMMA, and ZEP), and this sets limitations

for the resolution of chemically amplified resists. Some of the factors inducing LER are listed as follows[4]:

1. Acid gradients at exposed/unexposed interfaces

2. Trace amounts of background acid in "unexposed" regions becoming larger at lower k_1

3. Acid diffusion during post-exposure bake

4. Swelling and statistical dissolution effects at line edge

5. Shot noise

The model used by Hinsberg[2] *et al.* for poly hydroxyl styrene (PHS) resist includes two main contributors that limit resolution:

i) Deprotection chemistry occurring outside of exposed areas

ii) Diffusion of photogenerated acid

For sub 50 nm, it is the photoacid diffusion that dominates the limitation in resolution.

The highest resolution in chemically amplified resist is achieved by using low activation energy protecting groups[5]. Resolution down to 30 nm is demonstrated by using e-beam exposure of a PHS with a low activation energy protection group bonded to the polymer. However, it is not clear whether this approach can be extended to sub-20 nm resolution or not.

Because the variations in line width will impact saturation current and off state current in sub-0.1 μm MOSFETs (see Fig. 1.1), low LER is one of the main requirements for future resist chemistries and should be explored in more detail[6][7]. LER is related to many process variables like baking, development conditions, and also to resist properties like polymer structure, loading of photo acid generator (PAG) and base quencher. LER is inversely proportional to exposure dose, image log slope (ILS), and resist contrast. [6], [7] have a vast amount of information on interactions and contributors of LER and image blurring.

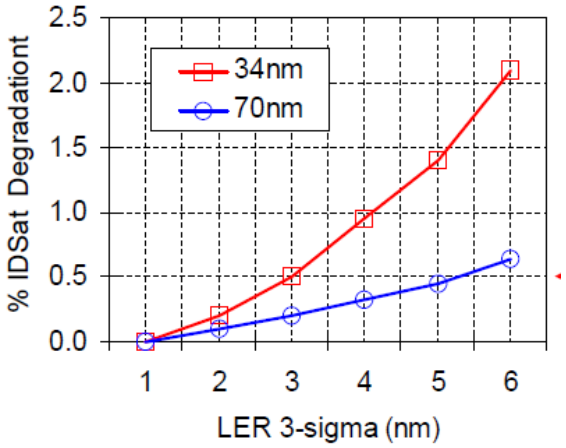

Figure 1.1 Saturation current degradation for 70 nm devices (130 nm technology) and 34 nm devices (80 nm technology) as a function of LER[7].

Gronheid[8] *et al.* compared imaging performance of chemically amplified resist (EUV-6) and non-chemically amplified resist (PMMA). Their studies showed that the resolution and image quality of PMMA is superior to that of CAR as shown in Fig. 1.2[8]. The exposure dose for printing dense patterns shown in Fig. 1.2 (a) is varied from 150 mJ/cm^2 to 550 mJ/cm^2. PMMA shows good contrast and sharp side wall slopes as in Fig. 1.2 (a). Even though, CAR requires much less exposure dose to print similar size patterns, images suffer from LER as shown in Fig. 1.2 (b). It is not possible to print dense patterns at 25 nm half pitch (hp) with EUV-6. The severe blurring of the latent image during PEB is evident from Fig. 1.3[8].

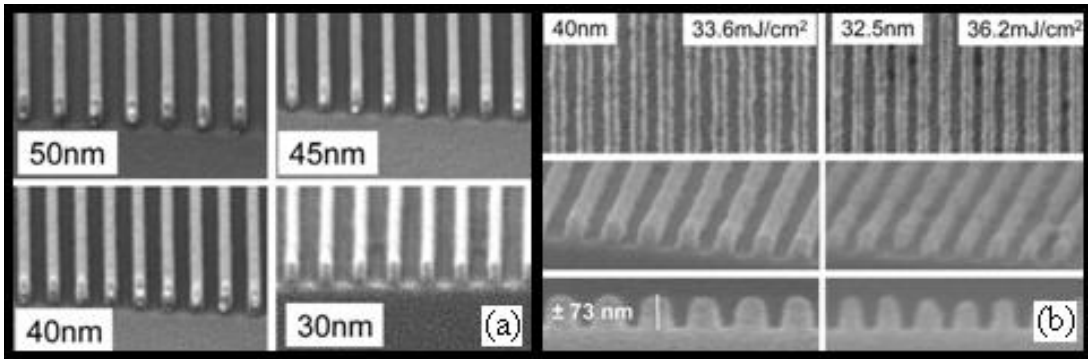

Figure 1.2 (a) SEM images of dense patterns with PMMA (indicated numbers are half pitch values), and (b) SEM images of dense patterns with EUV-6[8].

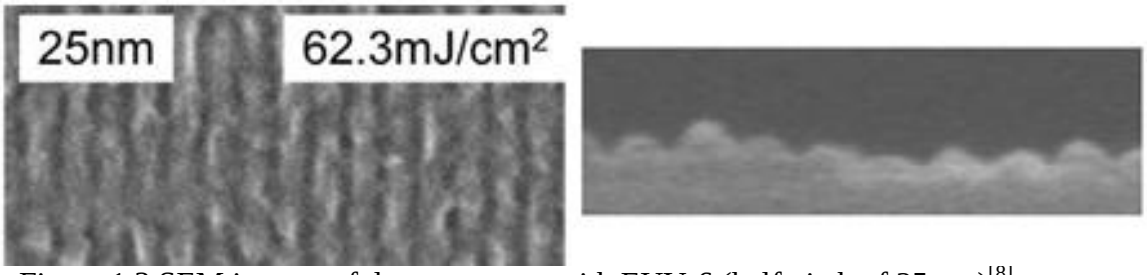

Figure 1.3 SEM images of dense patterns with EUV-6 (half pitch of 25 nm)[8].

1.2 Optical Materials for 193 nm Optics

Most widely used material for 193 nm optics is UV grade fused silica (UVGFS) that has a relatively low absorption (T internal ≥ 88% per cm at 185 nm) and thermal dispersion (dn/dT=20.6 ppm/K at 193.0 nm). Apart from the optical transparency and scattering of optical materials, minimizing any radiation induced changes in optical properties is also very crucial to ensure a long practical lifetime of the projection optics.

Compaction and color center formation were the primary concerns for laser induced damage in early fused silica optics[9]. Compaction causes wave front aberrations in the lens which is known to be a two photon process (TPP) type behavior in an excimer laser. At low levels, compaction induced effects increase linearly with the number of pulses, and at a parabolic rate with the intensity of an individual pulse[10]. As an early estimate, a lifetime around 10 years was predicted for 193 nm lithography fused silica lens for an energy density below 1 mJ/cm^2 per pulse within any element of the lens[11]. Such a restriction was definitely a driving force in choosing chemically amplified resist systems which require exposure doses less than 25 mJ/cm^2, based on a 50 wafer per hour throughput for 150 mm wafers. It was clear back then that high dose resist could be used only if calcium fluoride (CaF) is substituted at critical (high power) elements of the projection lens.

Impurity-free calcium fluoride lens materials possess excellent transmission characteristics at 193 nm. In addition, they do not suffer from compaction or rarefaction effects upon radiation that fused silica does. However, loss in transmission is observed in the existence of impurities like sodium or yttrium[12],[13]. Therefore, CaF should be very pure when it is used in an exposure system. Modern 193 nm systems have CaF components at critical locations that allow them to operate at high fluence levels. However, the large birefringence and degree of inhomogeniety limits the use of CaF to only a small number of elements.

1.3 ArF Excimer Laser Source Technology for 193 nm

Current excimer lasers run at repetition rates up to 6 KHz, with a pulse energy of 15 mJ[14]. Fig. 1.4 shows the product roadmap of the laser company, Gigaphoton, starting from 90 nm down to 32 nm DRAM technology nodes. The 193 nm laser introduced in 2008 (GT62A) runs at 90 Watts of power. This power is twice the power of the lasers introduced in 2005 (GT40A). Second generation laser that is going to be introduced in 2011 for EUV will work at 280 Watts of power.

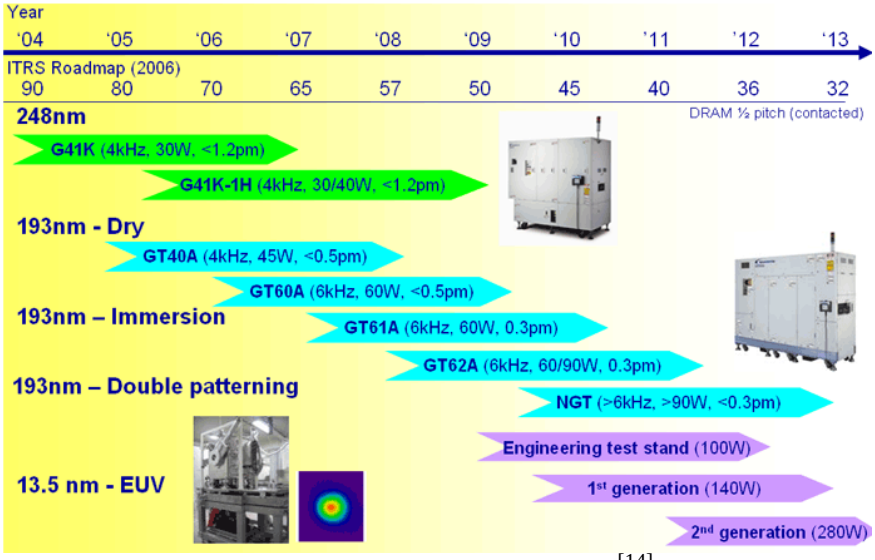

Figure 1.4 Gigaphoton product roadmap[14].

Following such a rapid improvement rate, laser power levels greater than 300 Watts is forecast in the near future. By employing multipass architecture, lasers can operate with better beam uniformity, and longer pulse width duration at a higher stability. The longer pulse duration will lower the possibility of thermally damaging the optics within the exposure system.

By combining high power lasers with CaF combined lens systems that will tolerate to high laser energy densities, wafer throughput can be increased or resist materials with lower sensitivities can be utilized instead of CAR. In this research, the latter option is investigated.

Chapter 2

Historical Review

2.1 Early 193 nm Resists

The high absorption values of novolac and polyhydroxystyrene groups at deep UV wavelengths have prevented them to be useful for 193 nm lithography. A research group at IBM came up with an "engineered" terpolymer in which each monomer served a specific purpose[15]. It was synthesized by free radical polymerization of methylmethacrylate (MMA), methacrylic acid (MAA) and t-butyl methacrylate (TBMA) as shown in Fig. 2.1. Upon radiation, the t-butyl group is cleaved off from TBMA via photogenerated acid, hence converted into MAA[15]. The photoproduct is very soluble in an alkaline developer.

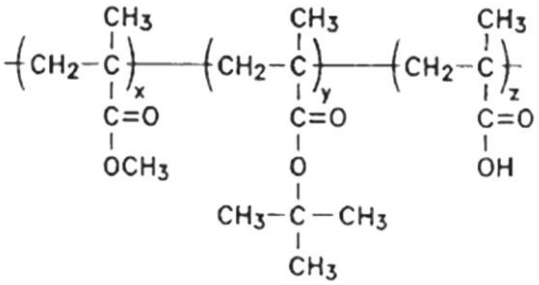

Figure 2.1 MMA-TBMA-MAA terpolymer chemical structure[15].

The IBM terpolymer has high sensitivity, low absorption at 193 nm (see Fig. 2.2) and also good thermal stability (Tg around 140°C-160°C) for single layer resist applications[16]. The degree of base solubility is easily adjusted by changing the molar fraction of methacrylic acid in the terpolymer. The plasma etch resistance has been increased to a level comparable the phenolic resins by incorporating alicyclic pendant groups into the resist.

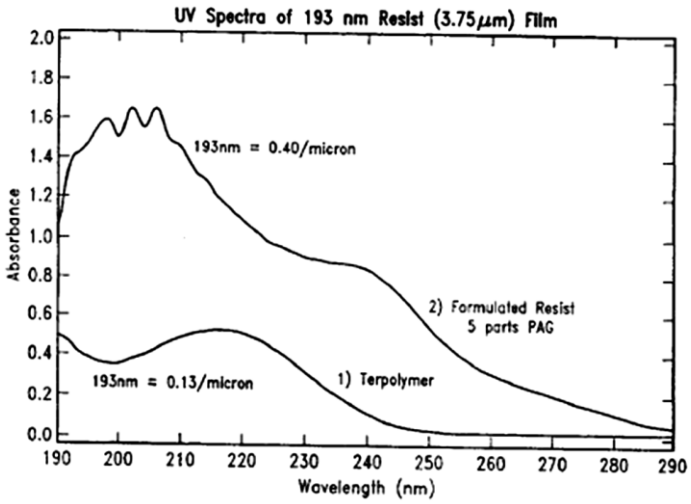

Figure 2.2 Absorbance spectrum of IBM terpolymer[16].

2.2 Modern 193 nm Resists

Most modern 193 nm CAR systems rely on polymerization of transparent acrylate backbones and addition of plasma etch resistant groups into the polymer chain. The addition of alicyclic pendant groups into the polymer has resulted in plasma etch resistance which is comparable to the phenolic-based resins[4]. Current 193 nm photoresists are mainly based on five platforms:

i. Methacrylate copolymers with alicyclic pendant groups (MA)
ii. Ring opening metathesis polymer (ROMP) with alicyclics in the main backbone
iii. Cyclo-olefin addition polymers (CO)
iv. Alternating copolymers of cyclo-olefins with maleic anhydride (COMA)
v. Vinyl ether/maleic anhydride (VEMA)

Among those five groups, MA, CO, and COMA are the most commonly used approaches. The concentration of protection groups is in the same range as in earlier versions (30-50 mol %).

The photoacid generators for early resists were based on trifluoromethanesulfonic acid (shortly, triflic acid). However, significant T-top formation resulted because of the volatility of triflic acid PAGs. In modern 193 nm resist systems, it has been replaced by heavier perfuoroalkyl sulfonates that have lower volatility, better resolution, and higher baking temperatures than triflic acid PAGs.

2.3 *O*-nitrobenzyl Chemistry as Dissolution Inhibitors

2.3.1 Review of *O*-nitrobenzyl Cholate Ester

In early 1980s, a novel two component resist system (base resin with dissolution inhibitor) has been introduced by Reichmanis *et al.* in Bell Laboratories. It is shown to be useful for sub-300 nm optical lithography due to high contrast and good resolution characteristics[17].

The base resin is a copolymer of methacrylic acid and methyl methacrylate, which is very transparent in deep UV wavelengths. The inhibitor is o-nitrobenzyl carboxylate ester that is initially insoluble in alkaline developer. However, upon radiation the ester cleaves into nitrisobenzaldehyde and carboxylic acid (photochemical reaction is shown in Fig. 2.3). The solubility in developer is achieved by this means[17].

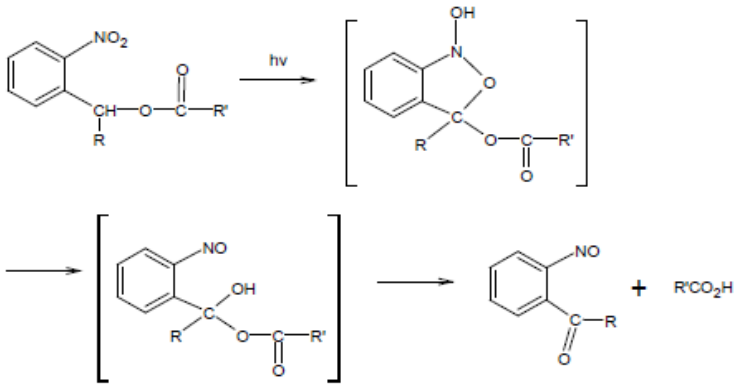

Figure 2.3 Photochemical reaction of o-nitrobenzyl ester upon radiation[17].

Reichmanis *et al.* synthesized a number of o-nitrobenzyl alcohol esters and examined their behavior individually in acrylic base resin. Table 2.1 shows the variation of inhibitor effectiveness with parent acid that is used in the esterification with the o-nitrobenzyl group. In this table, exposure time refers to the time necessary to completely remove the resist in the exposed regions with least possible thinning in the unexposed regions. 0.5 min corresponds to 100 mJ/cm^2. Contrast is found by taking the slope of the linear portion of the curves obtained by plotting the normalized thickness of the relief image as a function of log (exposure dose)[17].

Table 2.1 Variation of dissolution inhibitor effectiveness with parent acid of ester[17].

Parent acid	Developer[a]	% Thinning[b]	Exposure time[b] (min)	Contrast[b]
Adamantane Carboxylic acid	1	40	0.8	1.8
9-Fluorenone-4-Carboxylic acid	1	75	0.8	
Decanoic acid	2	60	0.8	1.6
12-Hydroxydodecanoic acid	1	50	0.6	1.7
N-Adamantylphthalamic acid	1	40	0.6	2.1
Cholic acid	3	20	0.5	2.0
Deoxycholic acid	3	20	0.6	2.0
Lithocholic acid	2	15	0.7	1.6
5β-Cholanic acid	2	25	0.8	1.5

[a] 1 = 10% aqueous $NaHCO_3$–Na_2CO_3 (9:1)
2 = 10% aqueous $NaHCO_3$–Na_2CO_3(9.5:0.5)
3 = 10% aqueous $NaHCO_3$
[b] in P(MMA-MAA) (7:3), $M_w = 50{,}760$, $M_w/M_n = 2.23$

It is seen from Table 2.1 that cholic acid, deoxycholic acid and lithocholic acid are the parent acids that give highest contrast with least thinning. Such bulky esters will undergo a greater change in solubility and form a more polar, aqueous alkali soluble acid upon radiation[17].

Choice of bulky groups for dissolution inhibition has its advantages. Because of their large size, they are able to protect base resin from developer attack more efficiently. The larger

the volume fraction of the matrix that has been converted to soluble state by a photochemical reaction, the fewer photons required and the higher the sensitivity is[17].

Considering previous discussions about the parent acid (Table 2.1), cholic acid is a good choice for esterifying the o-nitrobenzyl group. The resulting inhibitor that is synthesized from cholic acid and ortho-nitrobenzyl group is called "o-nitrobenzyl cholate".

The resist properties of nitrobenzyl cholate systems can be varied by adding substituents as shown in Fig. 2.4. Trimethylsiyl, acetyl, trifluoroacetyl, and pivaloyl groups can be substituted for hydroxyl groups (R1, R2, and R3). The hydrophobicity of the inhibitor increases as the number of hydroxyl groups attached to the sides is reduced[17].

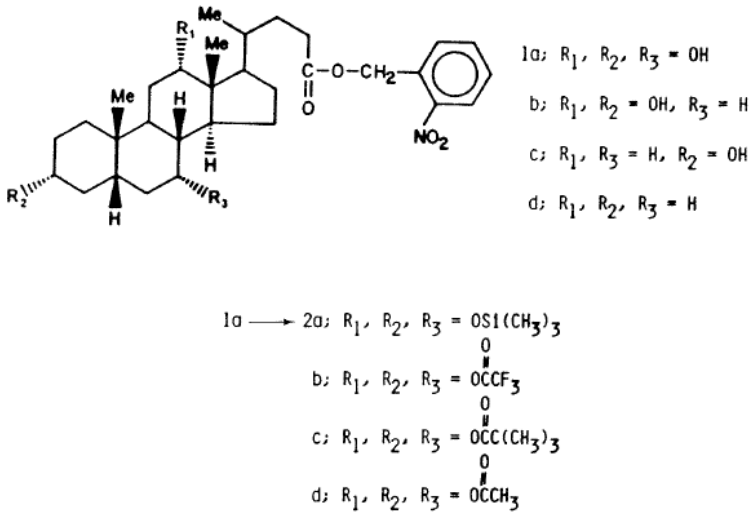

Figure 2.4 Scheme illustrating the structures of substituted o-nitrobenzyl cholate[17].

Table 2.2 shows this behavior in "% Thinning" column which gives percent dark loss for five different cases. Hydroxyl groups allow the developer to penetrate to the unexposed part of the film and result in a loss in the discrimination of solubility between exposed and unexposed regions. Investigating Table 2.2 and Fig. 2.5 shows that the highest contrast (greater than 4) is achieved if pivaloyl groups are attached as substituents[17].

Table 2.2 Substituent effects on dissolution inhibitor effectiveness[17]

Cholate derivative	Developer[a]	% Thinning[b]	Exposure time[b] (min)	Contrast[b]
Tris-trimethylsilyl	1	25	0.5	2.3
Tris-trifluoroacetyl	1	20	0.5	2.5
Diacetyl	2	8	0.5	2.3
Triacetyl	3	0	0.5	3.2
Tripivaloyl	4	0	0.5	>4

[a] 1 = 10% aqueous $NaHCO_3$
2 = 10% aqueous $NaHCO_3$–Na_2CO_3 (9.5:0.5)
3 = 10% aqueous $NaHCO_3$–Na_2CO_3 (9:1)
4 = 10% aqueous $NaHCO_3$–Na_2CO_3 (1:1)
[b] In P(MMA-MAA) (7:3), $M_w = 50{,}760$, $M_w/M_n = 2.23$

Characteristic curves that are obtained for P(MMA:MAA) (7:3) is given in Fig. 2.5 for o-nitrobenzyl-cholate ($R_1 = R_2 = R_3 = OH$), o-nitrobenzyl *O,O*-diacetyl-cholate, *O,O,O*-triacetyl-cholate, and *O,O,O*-tripivaloyl-cholate. Exposure dose is given in seconds and 30 sec corresponds to 100 mJ/cm^2[17].

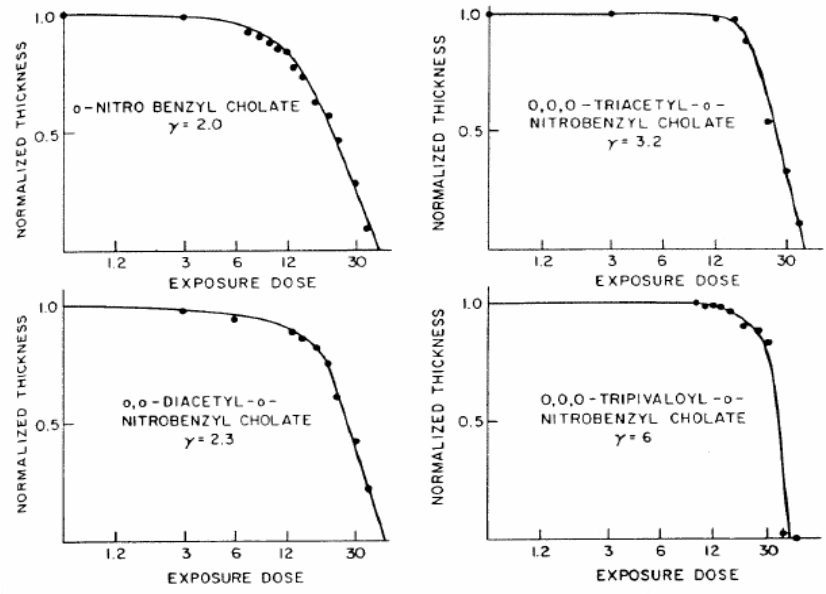

Figure 2.5 Characteristic curves for substituted nitrobenzyl cholate esters[17].

Poly(MMA-co-MAA) is a very suitable choice as the base resin due to its adjustable solubility in aqueous base solutions and low deep UV absorbance. Fig. 2.6 compares the optical spectra of o-nitrobenzyl cholate (NBC) in novolak and P(MMA:MAA) (7:3)[17].

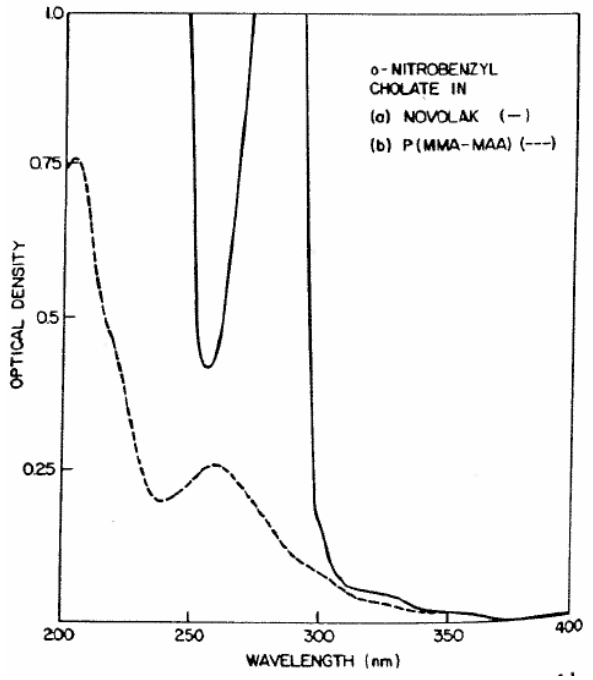

Figure 2.6 Absorbance of NBC in (a)Novolak and (b)P(MMA-co-MAA)[17].

The ratio of methacrylic acid in the copolymer composition is shown to impact resist characteristics significantly, so do the molecular weight and polydispersity. Table 2.3 shows that (7.5:2.5) is the optimum (MMA:MAA) ratio for weak alkaline developing conditions. Low content of methacrylic acid prevents even a strong alkaline aqueous developer from delineating an image. Polymer matrices of high molecular weights result in poor sensitivity, and low molecular weight result in substantial thinning as shown in Table 2.4[17]. Table 2.4 indicates that for the development conditions Reichmanis *et al.* used, polymer molecular weight between 40 k and 90 k and low polydispersity (around 2.0, or 2.2) gives best results.

Table 2.3 Effect of methacrylic acid content on the resist properties[17].

MMA-MAA[a] Mol ratio	Molecular weight (× 10⁻³)	M_w/M_n	Developer[b]	Exposure time (min)	Contrast
4.5:5.5	322	2.8	$NaHCO_3$[c]	—[e]	—
7:3	51	2.2	$NaHCO_3$[d]	0.5	2
7.5:2.5	67	2.0	Na_2CO_3[d]	0.6	10
8:2	59	2.3	1*N* NaOH	—[f]	—
8.3:1.7	108	2.6	1*N* NaOH	—[f]	—

[a] Containing 20 w/o o-nitrobenzyl cholate.
[b] Followed by a 30 sec H_2O rinse.
[c] 5% aqueous solution.
[d] 10% aqueous solution.
[e] Entire film removed on development.
[f] No pattern is delineated upon exposure and development.

Table 2.4 Effect of polymer molecular weight on the resist properties[17].

P(MMA-MAA) (7.5:2.5)		Required exposure in mJ/cm² as a function of developer[b]			Thickness remaining (%)
MW × 10⁻³	M_w/M_n	10% aq. Na_2CO_3 (time)	10% aq. K_2CO_3 (time)	AZ(1:1) (time)	
36	3.8	100 (60 sec)	90 (45 sec)		25
67	2.0	125 (3 min)	150 (2 min)	50 (60 sec)	100
89	2.2	160 (3 min)	190 (2 min)	200 (60 sec)	100
290	2.0	>500 (10 min)	>500 (10 min)	450 (2 min)	100

[a] Containing 20 w/o o-nitrobenzyl cholate, initial thickness 8000-8500A.
[b] Followed by a 30 sec H_2O rinse.

Finally, Table 2.5 shows the effect of dissolution inhibitor loading varying between 10 % and 30 %. A higher concentration of the inhibitor will require extended exposure time and degrade sensitivity, whereas a lower content will cause substantial thinning[18].

Table 2.5 Effect of o-nitrobenzyl cholate concentration on resist performance[18].

Weight percent inhibitor	Developer	Sensitivity (mJ/cm²)	Contrast
10	Na_2CO_3[c]	130	>10
20	Na_2CO_3[c]	160	>10
30	Na_2CO_3[c]	180	>10

[a] o-Nitrobenzyl cholate in P(MMA-MAA)(7.5:2:5), MW = 89 × 10³, initial thickness, 8000A.
[b] 2.5% aqueous solution, development time of 3 min, followed by a 30 sec H_2O rinse.
[c] 10% aqueous solution, development time of 3 min, followed by a 30 sec H_2O rinse.

Comparison of quantum yields for o-nitrobenzyl cholate esters in P(MMA-MAA) matrix is given in Table 2.6. Highest quantum yields are achieved for o,o'-dinitrobenzyl cholate and α-methyl-o-nitrobenzyl cholate, with values of 0.20 and 0.18 at 254 nm, respectively[19].

Table 2.6 Quantum yields of the photochemical reaction for cholate esters[19].

Material[a]	Φ (254 nm)	Φ (313 nm)
o-Nitrobenzaldehyde	0.45 (0.48)[b]	0.57 (0.50)[c]
o-Nitrobenzyl cholate	0.07	0.17
o,o'-Dinitrobenzyl cholate	0.20	0.28
o-Methoxy-*o'*-nitrobenzyl cholate	0.12	0.17
p-Methoxy-*o*-nitrobenzyl cholate	0.14	0.16
o-Cyano-*o'*-nitrobenzyl cholate	0.01	<0.005
p-Methoxycarbonyl-*o*-nitrobenzyl cholate	0.07	0.07
α-Methyl-*o*-nitrobenzyl cholate	0.18	0.15
Poly(*o*-nitrobenzyl methacrylate)	0.04	0.06

[a] 20 wt % in P(MMA-MAA) (7.5:2.5) M_w = 67,000, M_w/M_n = 2.0.
[b] In a polycaproamide film
[c] In a PMMA film

The quantum yield of the photochemical reaction usually reflects the sensitivity of the resist system; however, for o-nitrobenzyl cholate esters the value of the quantum yield proves loose correlation. There is an additional mechanism that helps to increase the solubility of the resist after exposure[19]. Table 2.7 shows that the molecular weight of the polymer is halved after irradiation. Low absorbance value of P(MMA-co-MAA) at 260 nm indicates that this cannot be direct polymer photodegradation. So, the nitrobenzyl ester is believed to be acting as a radical source to cause main chain scissioning to occur in the base polymer.

Table 2.7 Photodegradation of P(MMA-co-MAA) upon radiation[19].

	Polymer molecular weight			
	Before irradiation		After irradiation	
Resist	M_w	M_w/M_n	M_w	M_w/M_n
o-Nitrobenzyl cholate-P(MMA-MAA)	73100	2.76	32700	2.2
	71500	2.88	37000	2.82

2.3.2 Use of *O*-nitrobenzyl Cholate System

O-nitrobenzyl cholate ester is used to realize a two component resist system for 193 nm lithography. The first base resin tested is the optically transparent and aqueous alkaline soluble P(MMA-MAA) copolymer. Other resist systems are also investigated and the experimental results collected are given in following chapters. Since there is no volatile photoproduct upon radiation, such a non-CAR system can be used for 193 nm immersion lithography as well.

Substituents on the esters have shown to have a huge impact on the resist properties. Thinning, sensitivity, and optical absorbance are all dependent on those substituents. It is seen from the experiments conducted in Bell Labs that for least thinning and highest contrast, pivaloyl group should be attached to the cholate on three *ortho* positions.

Bile acid esters have a high alicyclic carbon content that results in some degree of reactive ion etch (RIE) resistance (Petrov *et al.* (2004), Allen *et al.* (1995)). However, substituting trimethylsiyl group to one of the hydroxyls might be another option to further increase the plasma etch resistance. There is a huge room of flexibility in the functionalization of cholate esters.

With the published data in literature, it is known that *o,o*-dinitrobenzyl cholate and α-methyl-o-nitrobenzyl cholate have higher quantum yield than o-nitrobenzyl cholate. So, experimenting on substituted o,o-dinitrobenzyl cholate instead of o-nitrobenzyl cholate can be another extension of this research. The recipes to synthesize o-nitrobenzyl cholate inhibitor and its derivatives are given in [20].

2.4 Review of Terpolymer of Maleic Anhydride, Norbornene, Acrylic Acid

During late 1990s, Houlihan and his coworkers studied the terpolymer of norbornene (NB), maleic anhydride (MA) and acrylic acid (AA), known as poly(NB/MA/AA) and shown in Fig. 2.7, for 193 nm and 248 nm lithography systems. They blended t-butyl cholates (chemical amplified version of cholate ester) with poly(NB/MA/AA) at different acrylic acid concentrations in which PAG was used to cleave the t-butyl group from cholate part so that the solubility of the photoresist in alkaline developer was achieved upon exposure. Using this terpolymer, they were able to print 0.27 μm L/S pattern with good photosensitivity (9 mJ/cm^2) due to chemical amplification kinetics[21]. P(NB/MA/AA) is explored in this research as a potential base resin. The details of material synthesis and experimental results are given in following sections.

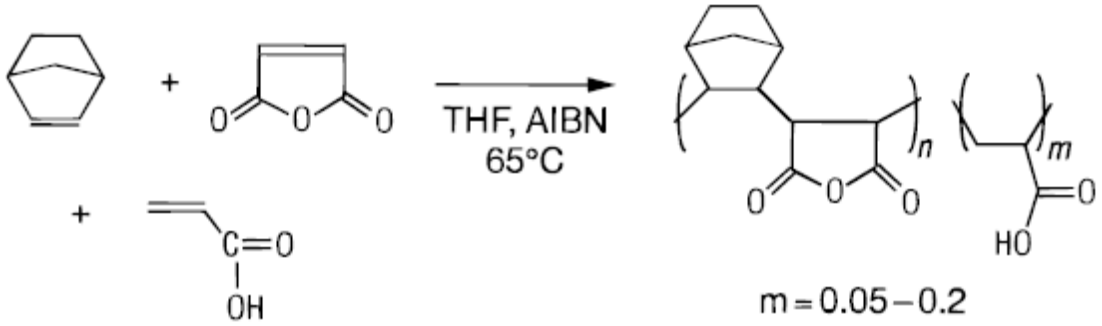

Figure 2.7 P(NB/MA/AA) chemical structure[21].

2.5 Review of PNBHFA Homopolymer

The use of hexafluoroisopropanol (HFA) group as the acidic moiety in an alkaline developable polymer system has received a great deal of attention since it was first proposed for 193 nm lithography by Ito *et al*. in 1997[22],[23]. Replacement of carboxylic acid with HFA offers

several advantages like high optical transparency, reduction of swelling, good lithographic performance, etc[23].

Even though the homopolymer (PNBHFA, shown in Fig. 2.8) synthesized by polymerizing norbornene hexafluoroalcohol (NBHFA) with Pd or Ni catalyst has a pKa similar to that of PHOST; the dissolution characteristics are very different from that of the phenolic counterparts.

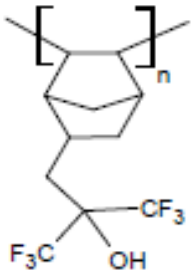

Figure 2.8 PNBHFA Chemical Structure.

Ito and his coworkers found that the dissolution rate of PNBHFA in 0.21N TMAH is 400 nm/sec, which is much faster than the dissolution rate of PHOST. It is also shown that the dissolution rate is not affected by the molecular weight of the polymer which is counterintuitive. The endo/exo ratio in PNBHFA has a big impact on the dissolution kinetics as shown by Fig. 2.9[24]. Higher exo content in PNBHFA results in lower dissolution rate. From their imaging studies, Ito and his coworkers showed that higher resolution is achieved for exo-enriched PNBHFA. They were also able to print dense features with 120 nm half pitch by using PNBHFA as a contrast enhancer for a conventional resist material.

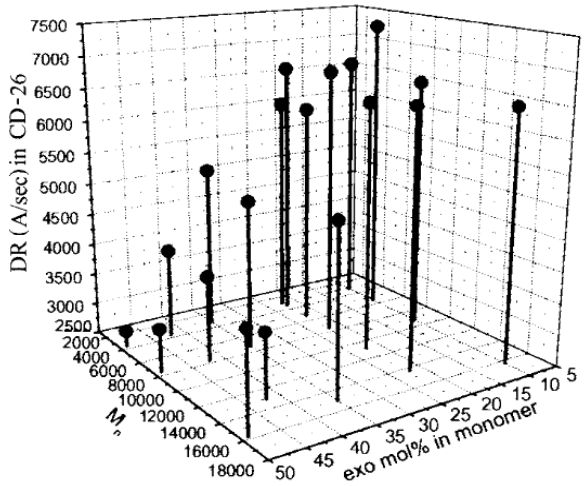

Figure 2.9 DR of PNBHFA in 0.26N TMAH versus M_n and % exo concentration[24].

From their extensive studies on NBHFA derivatives, Ito and his friends derived the following important conclusions:

- DR of PNBHFA in 0.26 N CD26 is somewhat linear (3,000-8,000 A/sec) and not affected by the molecular weight of the polymer.
- Dissolution behavior of PNBHFA in a weaker developer (e.g. 0.21 N) is not linear and composed of several stages. Dissolution stages involve swelling and gel layer formation. That makes one to be cautious when reporting the DR for PNBHFA.
- DR of PNBHFA depends on the overall polymer structure and is not governed entirely by pKa of the resist.
- Certain PAGs strongly inhibit the dissolution of PNBHFA; however, exposure does not increase the dissolution rate of the resist material as it does for a conventional resist system.
- Exo isomer interacts with a PAG or dissolution inhibitor more strongly than endo.

Chambers *et al.* investigated the blends of PNBHFA with dissolution inhibitors for 157 nm lithography in 2003[25]. One of the main findings of their study is the remarkable

dissolution inhibition properties of PNBHFA resist. They found that the dissolution inhibition response of PNBHFA to a dissolution inhibitor was typically an order of magnitude better than novolac resin to the same inhibitor as shown on Fig. 2.10. The imaging capability of a two component resist system utilizing PNBHFA as the resist matrix is shown to be very promising.

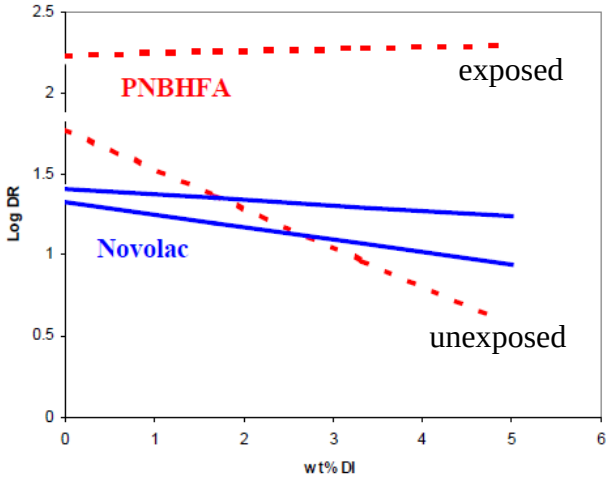

Figure 2.10 Meyerhofer plot of a carbonate based DI in PNBHFA and Novolac[25].

Under the guidance of previous work done on the norbornene hexafluoroalcohol derivatives, nitrobenzyl cholate inhibitors are tested at different loading ratios. The PNBHFA polymer is donated by Promerus LLC (Brecksville OH), and experimental results are given in the following sections.

Chapter 3

Methods

The synthesis, testing and characterization of materials are carried out as follows to evaluate dissolution properties, optical absorption spectra, sensitivity, contrast, and lithographic performance at 193 nm.

For synthesis of some of the base resin and dissolution inhibitors, Imaging Materials Lab in Building 76 at Rochester Institute of Technology (RIT) campus is used. DNQ is donated by AZ Chemicals and the homopolymer of polynorbornene hexafluoro alcohol (PNBHFA) is donated by Promerus LLC (Brecksville OH). The required equipment and chemistry is purchased from commercial suppliers (e.g. Sigma Aldrich, Alfa Aesar). Following material synthesis, characterization of the products is performed. Some specific methods include:

A. Material Casting and Film Forming: The optimum casting solvent is selected from widely used conventional solvents like PGMEA, ethyl lactate, cyclopentanone, etc. The % loading of polymer is less than 10 % by weight to achieve thin films. Spin coating is performed by CEE Spin Coater at spin rates that allow film thicknesses less than 100 nm.
B. Measurement of Cauchy Parameters: A, B, and C parameters of resist materials is measured using VASE (Variable Angle Ellipsometer). Those numbers are used to create recipes on Spectramap FT500 for thickness measurements.
C. Measurement of Spectroscopic Optical Properties: The absorbance of resist materials should not exceed ~8 /um (calculation via simulation in ProLITH assuming double patterning scenario, 22 nm line on a 88 nm pitch, 193 nm, 1.35 NA, polarized dipole 0.8/0.1, 55 nm LPM resist, no diffusion, index = 1.71, contrast = 10). Since the base resin is very transparent, the loading ratio of inhibitors should be carefully adjusted. In order to

measure the optical absorbance of resist materials, Perkin-Elmer UV-Vis Spectrophotometer is used.

D. Film Dissolution: The solubility of coated films is tested by weak and strong alkaline developers. Aqueous solutions of NaOH and TMAH are used at different concentrations. $NaHCO_3$ seems to cause scumming, hence avoided for this study. The dark loss should be less than 10 % with respect to the initial film thickness. The goal was to eventually use 0.26 N CD26 as the developer for new resist systems. Solvent based developers are avoided in this study.

E. Sensitometric Evaluation: The characteristic curves are generated after selecting the optimum development conditions. Exposures are carried out by using open frame 193 nm ArF laser by covering a broad range of doses.

F. Imaging Quality: The Amphibian XIS is used to expose coated wafers to print dense features at different pitch values. The quality of imaging is evaluated by SEM imaging.

Chapter 4

Experimental Results

4.1 Studies on P(MMA-co-MAA) Matrix

The first base resin studied in this research is the copolymer of methyl methacrylate (MMA) and methacrylic acid (MAA). Following subsections include data collected regarding the blends of this polymer and different dissolution inhibitors.

4.1.1 Synthesis and Evaluation of P(MMA:MAA) copolymer

The monomers (MMA, MAA) used in free radical polymerization are purchased from Sigma-Aldrich, USA. They are mixed (without further purification) at different molar ratios in a 1L round bottom flask with isopropanol (IPA) as the reaction solvent and AIBN (0.1 %) as the initiator. The copolymerization reaction was left to last for 16 hours in an oil bath set to 70°C with constant stirring, reflux condenser and thermometer[26],[28]. After reaction has stopped, the polymer is precipitated twice in hexane and dried in a vacuum oven at 100°C. Gel permeation chromatography (GPC) is used to measure the molecular weight and polydispersity (PD) of synthesized polymer. The data for four different lots is given in Table 4.1. The FTIR data of the synthesized copolymer is given in Fig. 4.1.

Table 4.1 Molecular weight and polydispersity data of synthesized copolymers.

(MMA:MAA) Ratio	M_w	M_n	PD
(65:35)	146 k	50 k	2.9
(70:30)	71 k	32 k	2.2
(75:25)	96 k	41 k	2.3
(85:15)	36 k	15 k	2.4

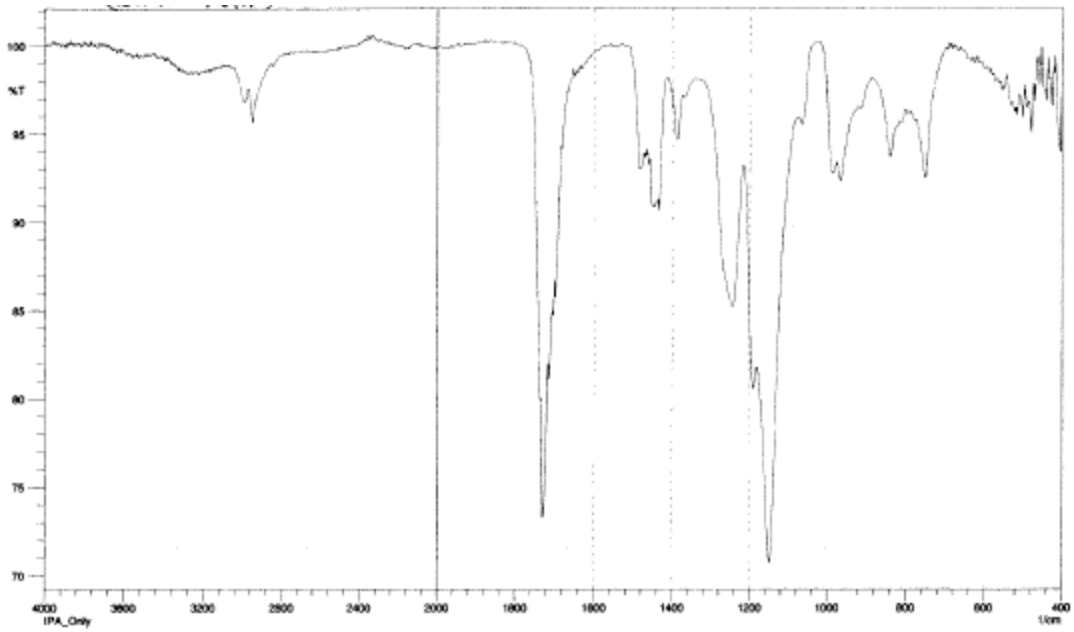

Figure 4.1 FTIR data of synthesized P(MMA-co-MAA) copolymer.

4.1.2 Synthesis and Evaluation of Cholate Inhibitor

O-nitrobenzyl cholate ester was synthesized from 2-nitrobenzyl bromide and cholic acid as given in [20]. After synthesizing nitrobenzyl cholate, its melting point is found to be around 199°C. However, it is reported to be between 211°C and 213°C in literature[20]. After purifying and recrystallizing the product, its melting point is increased to 213°C as predicted by [27]. The FTIR and H-NMR results corresponding to the purified o-nitrobenzyl cholate are given in Fig. 4.2.

4.1.3 Optical Characterization of Resist Materials

The P(MMA-co-MAA) is dissolved in cyclopentanone (3 % by weight), and then blended with dissolution inhibitors (20 % by weight with respect to the polymer weight). The solution is filtered several times through 0.45 μm filter and coated on silicon wafers to find

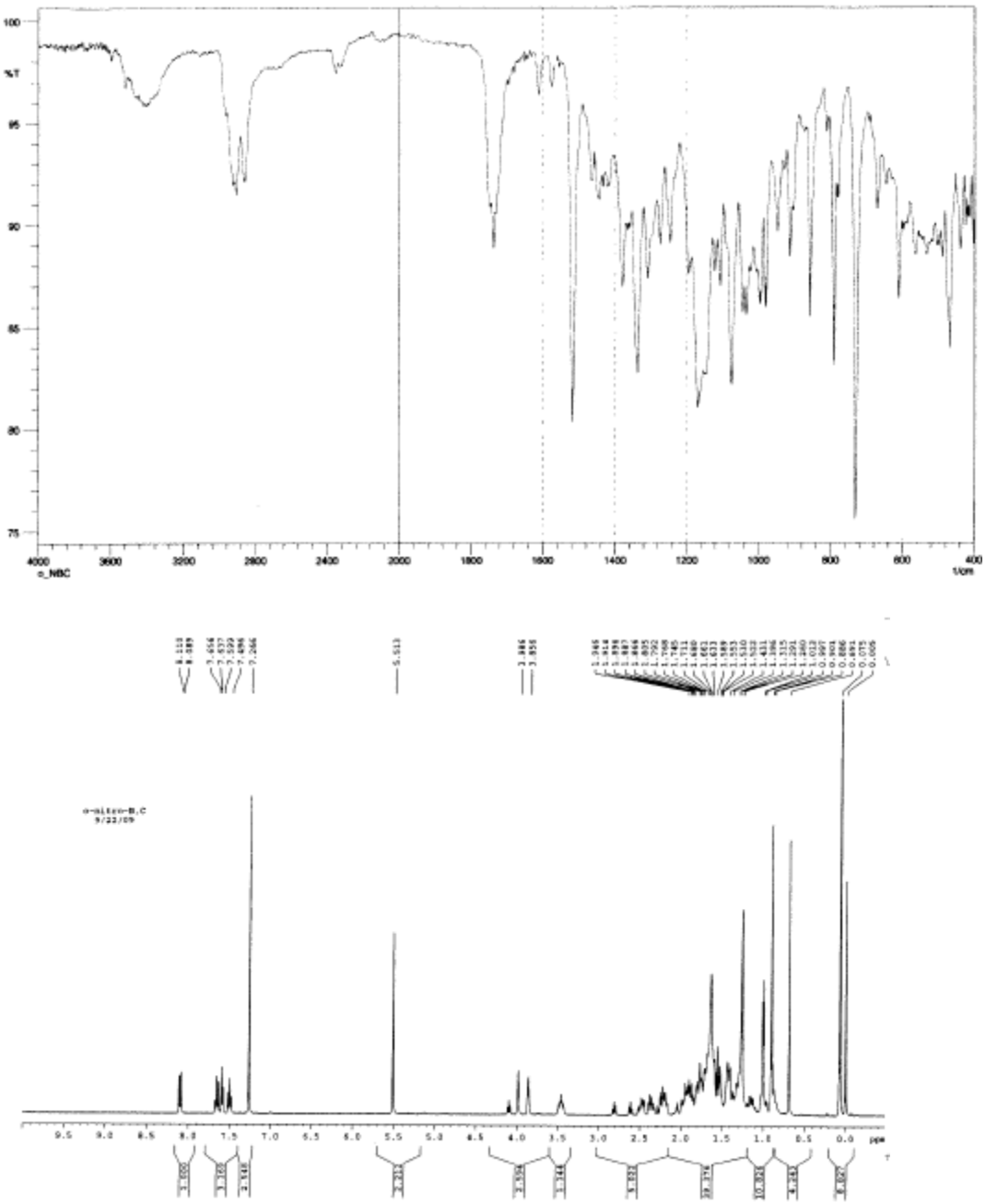

Figure 4.2 FTIR (top), and H-NMR (bottom) of synthesized o-nitrobenzyl cholate.

cauchy parameters of the control group (copolymer solution without inhibitor), MAA30NBC20 group (30 refers to the percent molar ratio of MAA in the copolymer, and 20 refers to the %

loading of the **N**itro-**B**enzyl-**C**holate inhibitor), and MAA30DNQ20. The wafers are prebaked before measurements at 160°C (for control group, and MAA30NBC20), and 110°C (for MAA30DNQ20). The data is given in Table 4.2.

Table 4.2 Cauchy parameters of P(MMA-co-MAA) resist materials.

	Control Group	MAA30NBC20	MAA30DNQ20
A_n	1.4893	1.4982	1.5363
B_n	1.0698e-3	2.4520e-3	-7.6505e-3
C_n	5.4896e-4	3.8665e-4	2.5975e-3

The optical absorbance spectrum of resist materials are calculated with Perkin Elmer Spectrometer from 190 nm to 380 nm. Each resist is spin coated on quartz wafers. The baseline is quartz wafer itself. It can be seen from Fig. 4.3 that when the loading ratio of all inhibitors are same (20 %), highest absorbance corresponds to DNQ blend.

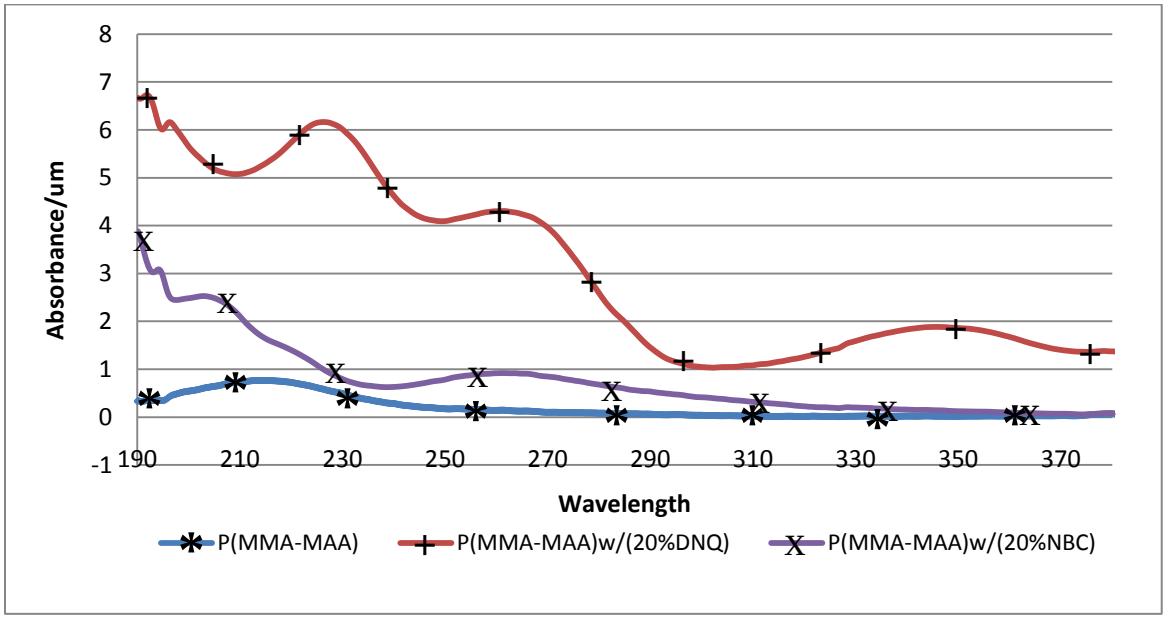

Figure 4.3 Absorbance of acrylate resist, with and without inhibitors as indicated.

Since the absorbance should be lower than 8 /um for a non-bleaching resist, loading of cholate inhibitors can be greater than 20%. Increasing the inhibitor content will call for higher exposure doses.

4.1.4 Dark Loss Study

Selection of the developer is the next step after optical characterization of resist samples. The development conditions should not cause significant amount of resist thickness loss in the unexposed regions, and yet should be strong enough to delineate image in the exposed regions. The maximum allowable dark loss is set to 10 % with respect to the initial thickness. The developer strength and development time is optimized to satisfy this criterion. Table 4.3 shows the dark loss study that was done with the copolymer that has 25 % methacrylic acid and 75 % methyl methacrylate (i.e. (MMA:MAA) with (75:25)). P(MMA:MAA) of (65:35) and (70:30) control groups are found to be extremely soluble in even a very weak alkaline developer (weak developer is defined as developer with pH around 8).

Table 4.3 Remaining thicknesses for resist samples after development. (Development: soak in developer as indicated time below, followed by water rinse)

Development (sec)	Control	MAA25NBC20	MAA25DNQ20
0 (initial thickness)	51 (nm)	63 (nm)	65 (nm)
10	20 (nm)	46 (nm)	62 (nm)
20	0 (nm)	34 (nm)	56 (nm)
30	0 (nm)	20 (nm)	48 (nm)

Copolymer with 15% acid ((MMA:MAA) with (85:15)) has very low solubility in alkaline solutions. For a strong alkaline developer (10% Na_2CO_3, pH around 12), there is no

dark loss after 15 sec soak in the developer followed by 30 seconds water rinse. However, the cholate samples and control groups show negligible amount of swelling.

4.1.5 Characteristic Curve Study

The characteristic curve study is done for 25 % and 35 % MAA copolymers and their blends with inhibitors as shown in Fig. 4.4 (L1 stands for Lot 1). Higher acid content in the base polymer results in a significant dark loss in alkaline developer compared to lower acid containing polymer. The thicknesses of MAA25, MAA25NBC20, MAA25DNQ, and MAA35 are 55 nm, 66 nm, 65 nm, and 60 nm, respectively.

The curves shown in Fig. 4.4 are obtained by open frame exposures on resist coated silicon wafers using 193 nm ArF laser. The exposed wafers are developed using a weak alkaline developer (15 sec soak followed by 30 sec DI water rinse).

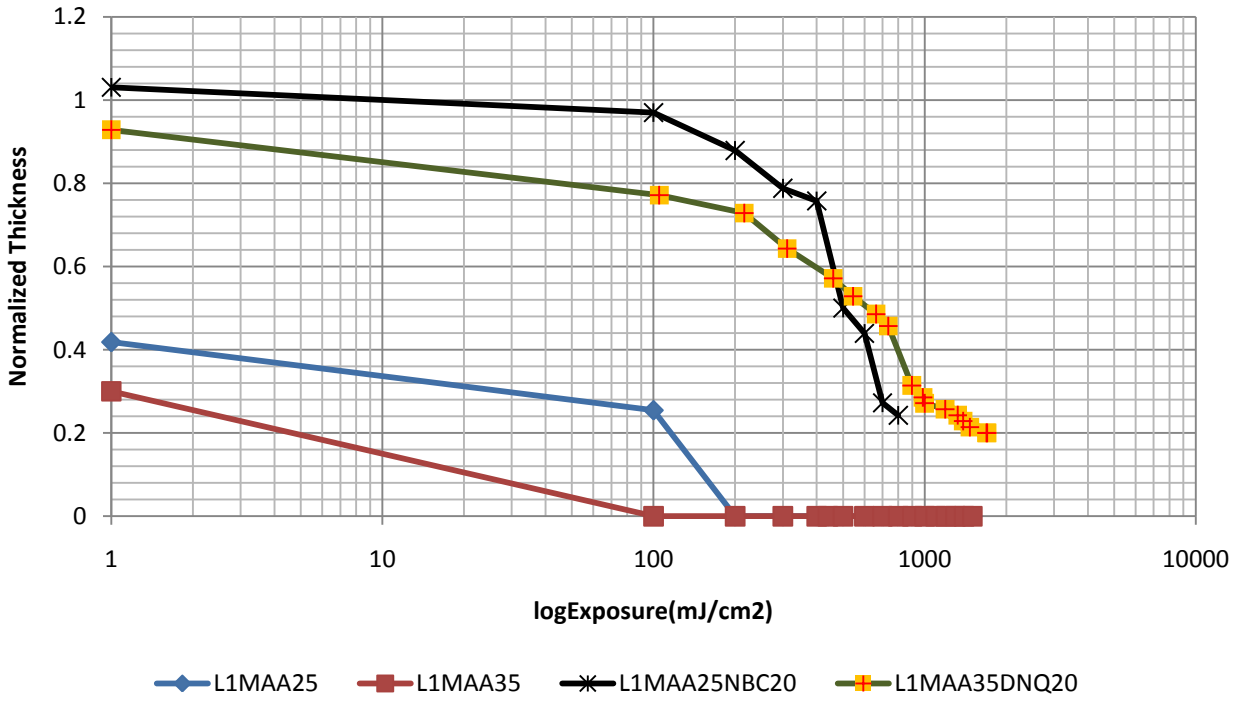

Figure 4.4 Characteristic curve study for 25 % MAA and 35 % MAA copolymers.

Sensitivity test for MAA15 lot has been done by using a stronger developer (10% Na_2CO_3 with pH of 11.9). E_0 for control group (MAA15) is around 450 mJ/cm^2 and for MAA15NBC20 around 220 mJ/cm^2.

4.1.6 Imaging Results

For imaging study, Amphibian XIS is set to 0.32 NA that prints 300 nm pitch dense patterns (150 nm lines/spaces). The processing conditions for this study are as follows:

i. Dehydration bake Si wafer at 200°C for 120 seconds

ii. Coat BARC (ARC 29A-8), bake at 200°C for 90 seconds

iii. Coat resist sample on BARC film (thickness less than 100 nm)

iv. Prebake at 160°C (or 145°C) for 120 seconds

v. Expose with 193nm laser (Amphibian XIS)

vi. Develop with a strong developer: NaOH (pH = 12), 15 sec soak in developer, 30 sec water rinse

Initial imaging studies are done on nitrobenzyl cholate wafers (MAA15NBC20). The first result observed under SEM was a very faint modulation at 120 mJ/cm^2 exposure dose (without a BARC layer underneath the resist) as seen on Fig. 4.5.

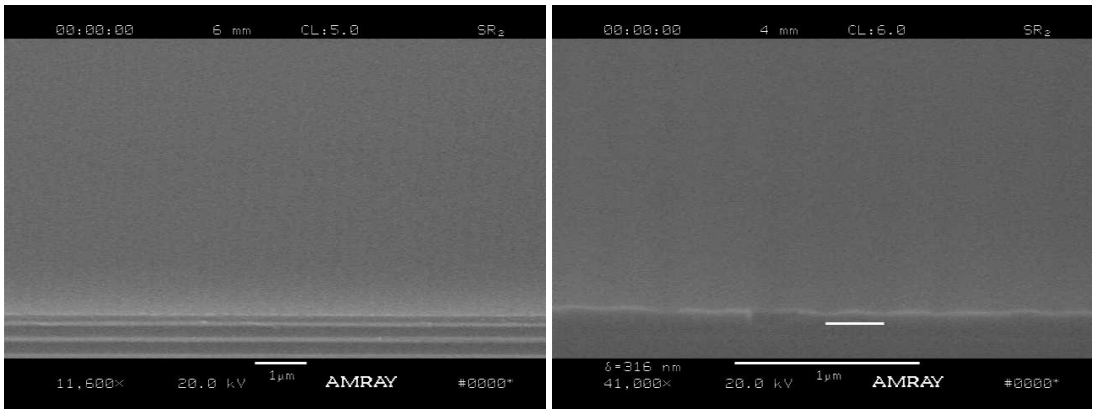

Figure 4.5 SEM image showing faint modulation for MAA15NBC20 (120 mJ/cm^2).

In order to minimize reflection at the resist and wafer boundary, BARC layer is coated underneath the resist. The best results for MAA15NBC20 lot is achieved when prebake temperature is 145°C (instead of 160°C) and with a BARC layer underneath the resist (Fig. 4.6). However, these images still show poor resolution for a resist that is designed to be used for state of the art technology nodes. In order to understand why the resolution is not good enough, imaging study is repeated for the control group (MAA15). The result is shown in Fig. 4.7 indicating that the resolution of cholate sample is limited by the resolution of base resin itself (i.e. acrylates type polymer). The nitrobenzyl cholate inhibitor seems to be increasing the photo-speed of the base resin by two times (250 mJ/cm^2 vs. 500 mJ/cm^2); but, the resolution of this system is limited by P(MMA:MAA) copolymer resin.

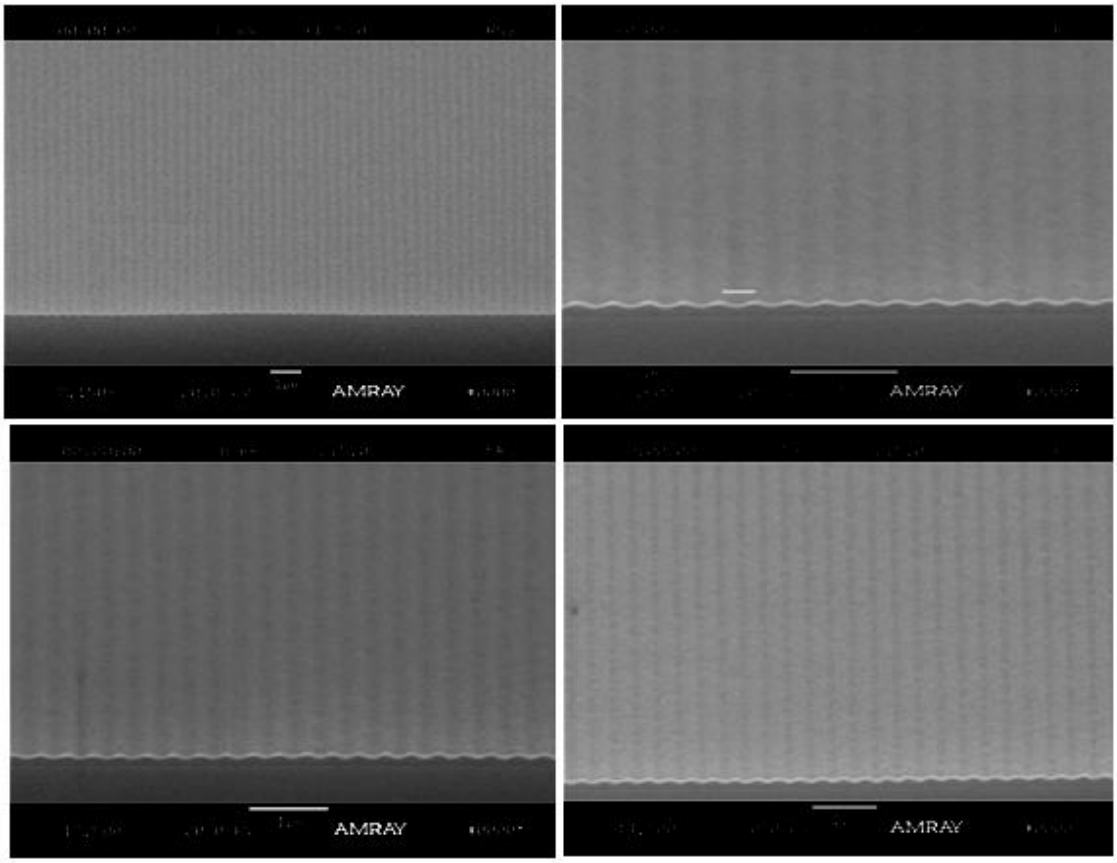

Figure 4.6 SEM image showing modulation for MAA15NBC20 (250 mJ/cm^2).

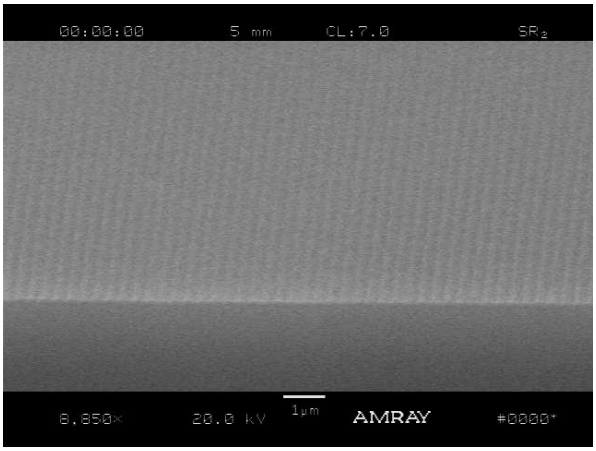

Figure 4.7 SEM image showing modulation for MAA15 (500 mJ/cm^2).

4.2 Studies on P(NB/MA/AA) Terpolymer Matrix

Initial imaging results on P(MMA-co-MAA) system indicated that the goal of this research will not be achieved with (MMA:MAA) copolymer system. One of the potential candidates that can be used as the base resin is the norbornene type polymers which also exhibits good dry etch resistance.

So, as the next step, two-component resist materials are prepared by using the same terpolymer that Houlihan and his coworkers used. The synthesis of P(NB/MA/AA), with (1/0.9/0.1) molar ratio, is carried out as described in (Wallow T.I., Houlihan F.M,. Nalamasu 0., Chandross E.A., Neenan T, Reichmanis E. SPIE, 2724, 355 (1996)). M_w, M_n, and polydispersity values are found to be 64,000 g/mol, 19,000 g/mol and 3.4, respectively. The synthesized polymer is blended with 30 % dissolution inhibitor and has dark loss much less than 10 % in diluted solutions of TMAH developer.

Three different resist samples are prepared by using P(NB/MA/AA) in cyclohexanone solvent (all 3 % by weight), one of them being the control group with no dissolution inhibitor and the other two having 30 % NBC and 30 % DNQ as the dissolution inhibitor. The cauchy

parameters are calculated as in Table 4.4. The spectroscopic study showed that the DNQ sample has very high 193 nm absorbance compared to the control and NBC group as shown in Fig. 4.8.

Table 4.4 Cauchy parameters of P(NB/MA/AA) terpolymer resist materials.

	Control Group	30% NBC Group	30% DNQ Group
A_n	1.5287	1.516	1.5425
B_n	4.651e-3	8.0553e-3	0.020909
C_n	-2.0889e-4	-3.0146e-4	-0.90304e-3

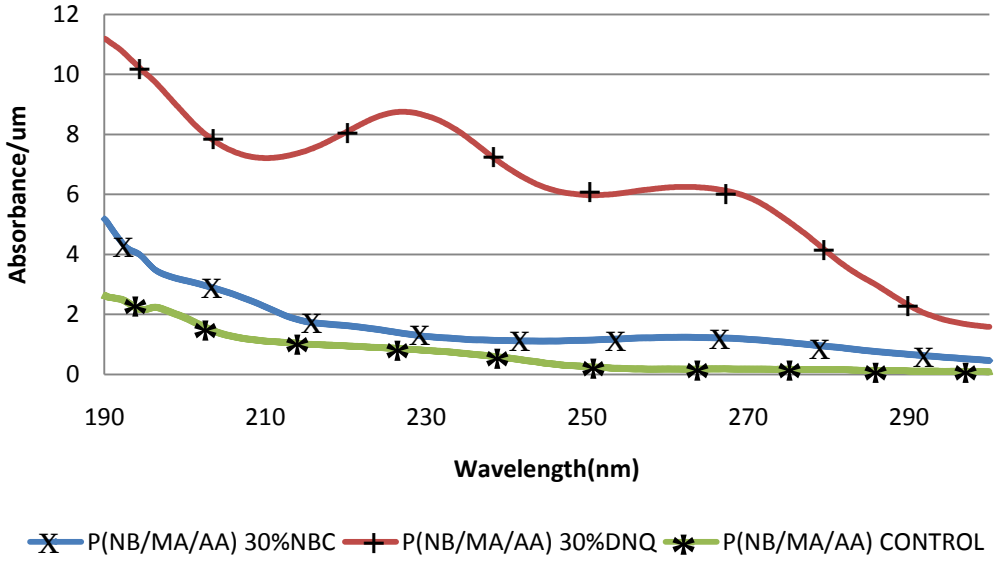

Figure 4.8 Optical absorbance of 30 % NBC and 30 % DNQ in P(NB/MA/AA) matrix.

During 193 nm open frame studies for contrast curve calculations, it is observed that the film exhibits severe cracking, peeling, and non-uniform dissolution characteristics (Fig. 4.9). The exposure dose for the Gaussian spot shown in Fig. 4.9 is 150 mJ/cm^2. The development was carried out by using 0.07 N TMAH solution (45 sec soak, followed by 15 sec water rinse).

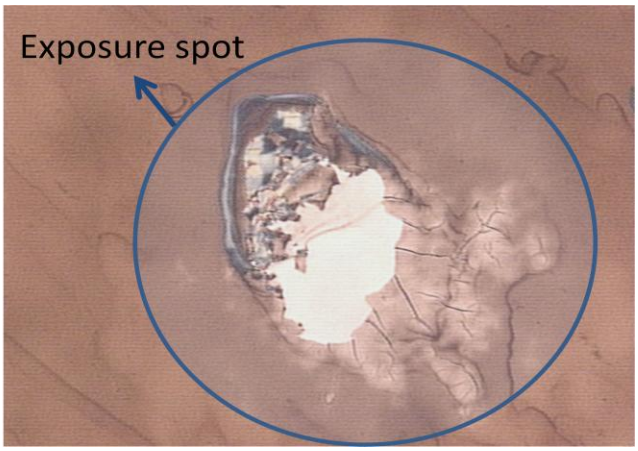

Figure 4.9 Exposed spot showing peeling, cracking for P(NB/MA/AA) with 30% NBC

Another problem encountered with this system is the hydrostability issue due to the maleic anhydride (MA) moiety. MA is prone to ring opening reaction in existence of water to form di-acid compounds, which increases the alkaline solubility and also limits its shelf life as a photoresist material. This is not tolerable for thin film resists applications. It is found from dark loss studies (done for 50 nm thick resist films) that even letting the resist solution to sit on shelf for 48 hours causes significant variation in dissolution behavior of P(NB/MA/AA) polymer. It is also found that 1 µL H_2O is more than enough to convert 16 ml of 3 % P(NB/MA/AA) (1/0.9/0.1) solution blended with 30% dissolution inhibitor from insoluble to soluble state. Due to these reasons, studies on P(NB/MA/AA) system are terminated.

4.3 Studies on Polymer of Norbornene Hexafluoro Isopropanol (PNBHFA)

The last base resin that is tested for this study is the homopolymer of norbornene hexa-fluoro alcohol, called PNBHFA. It was introduced very recently for 157 nm lithography but found to be a good candidate for 193 nm applications too. PNBHFA donated by Promerus has M_w of 10,000 g/mol and polydispersity of 2.0. The exo ratio is 20 % in the overall polymer structure.

4.3.1 Optical Characterization of Resist Materials

The PNBHFA is dissolved in cyclohexanone/MIBC mixture (3-5 % polymer by weight), and then blended with o-nitrobenzyl-cholate (NBC) at 20 % and 30 % loading concentrations. The solutions are filtered twice through 0.45 μm filter and coated on HMDS primed silicon wafers to find cauchy parameters for the control group (PNBHFA, without any inhibitor), PNBHFANBC*20* group (20 refers to the % loading of the **N**itro-**B**enzyl-**C**holate inhibitor), and PNBHFANBC*30*. The wafers are prebaked at 110°C for 90 seconds. The cauchy parameters are given in Table 4.5.

Table 4.5 Cauchy parameters of PNBHFA resist materials.

	PNBHFA	PNBHFANBC20	PNBHFANBC30
A_n	1.4512	1.4516	1.4616
B_n	3.2174e-3	2.6201e-3	3.8131e-3
C_n	-9.0456e-5	3.072e-4	7.3537e-5

The optical absorbance of resist materials are measured by Perkin Elmer Spectrometer from 190 nm to 300 nm. It can be seen from Fig. 4.10 even 30 % loading of NBC has 193 nm absorbance that is acceptable for very thin film lithography applications.

4.3.2 Dark Loss Study

In order to study the unexposed dissolution behavior of homopolymer and dissolution inhibitor blends in diluted TMAH solutions, HMDS primed silicon wafers were coated with PNBHFA control group and 20 % and 30 % NBC incorporated samples. The development time is kept to 15 sec, followed by 15 sec water rinse. The films thicknesses were less than 100 nm in

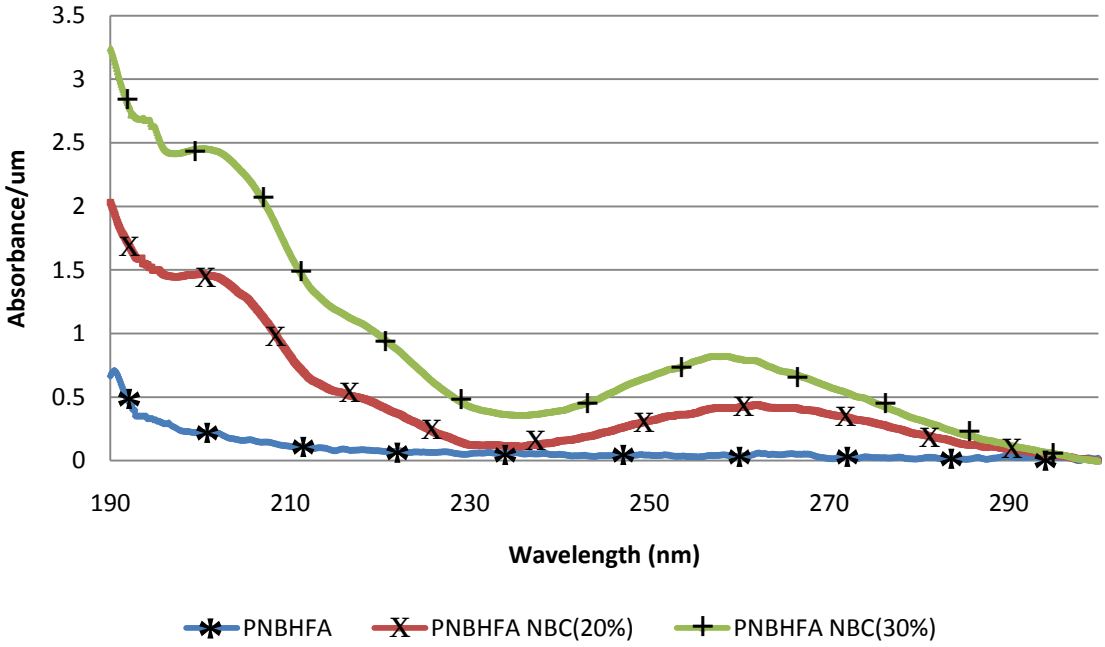

Figure 4.10 Absorbance spectra of nitrobenzyl cholate blends in PNBHFA matrix

each case, and normalized thickness loss is given in Fig. 4.11. It can be seen from this figure that the homopolymer itself is extremely soluble even in a diluted developer; however, its DI blends

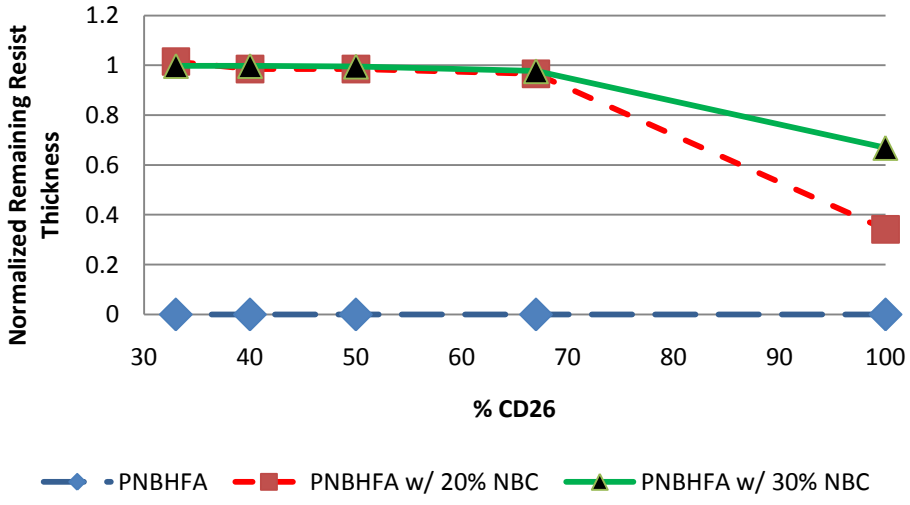

Figure 4.11 Effect of developer strength for unexposed PNBHFA and its DI blends

have much lower dissolution rates. The dissolution of these photoresist materials is not linear, in accordance with the published data in literature.

In Fig. 4.12 and Fig. 4.13, the thickness losses of unexposed PNBHFANBC30 and PNBHFANBC20 are given, respectively, as development time was varied from 10 sec to 60 sec for 0.26 N, 0.19 N, and 0.13 N TMAH developers. There is almost no dark loss for 30 % NBC loaded PNBHFA after 60 sec of soak in 0.19 N TMAH. The nonlinear dissolution kinetics is again evident in both cases.

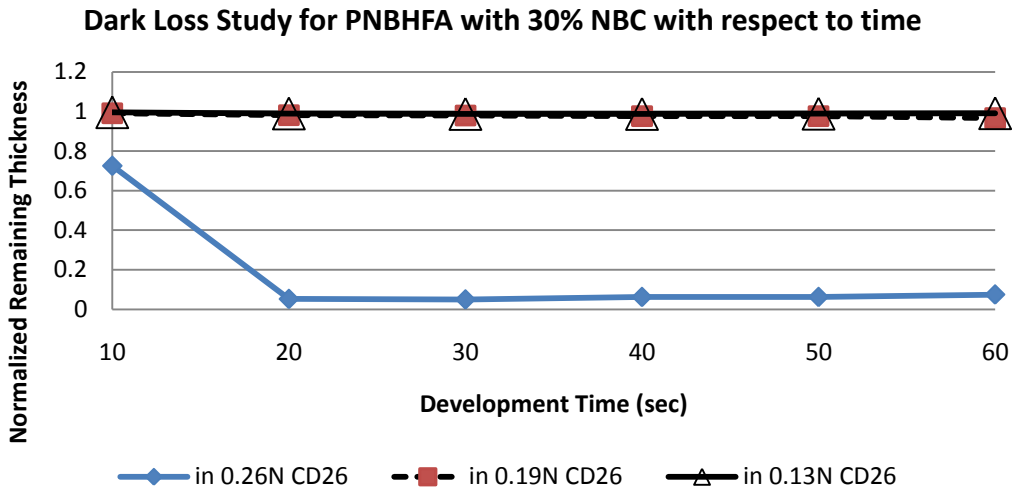

Figure 4.12 Thickness loss for PNBHFANBC30 vs. development time in three different normality TMAH developers.

4.3.3 Imaging Results

For imaging study, 193 nm laser is used at 0.32 NA, 0.39 NA and 0.53 NA to print 150 nm, 120 nm and 90 nm dense lines/spaces, respectively. The processing conditions for this study are as follows:

i. Dehydration bake Si wafer at 200°C for 30 seconds

ii. Coat BARC (ARC 29A-8)

iii. Bake at 200°C for 90 sec

iv. Coat resist on BARC (81 nm)

v. Bake at 110°C for 90 sec

vi. Expose with 193 nm laser (Amphibian XIS)

vii. Develop with 0.13 N TMAH , 15 sec water rinse

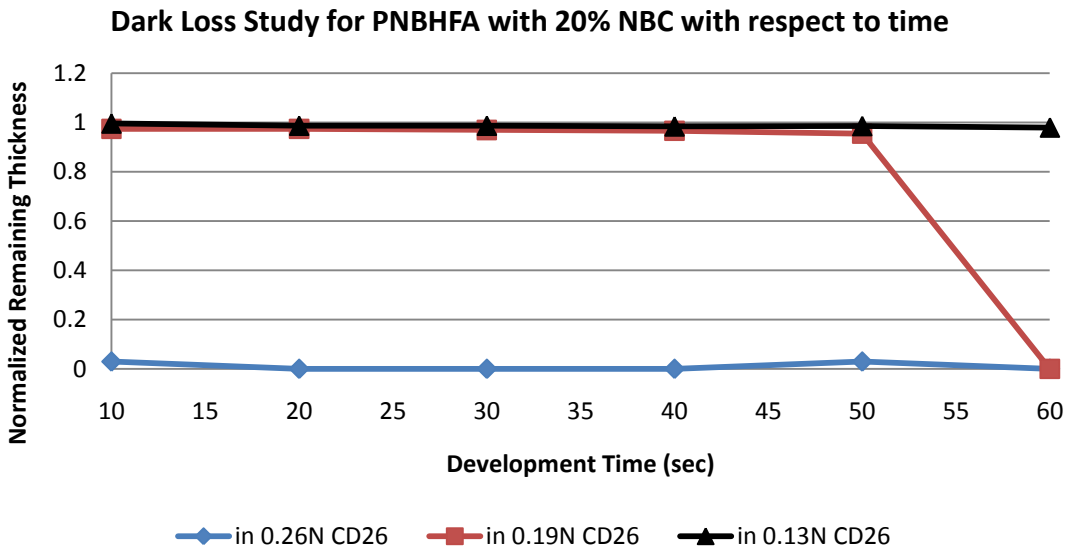

Figure 4.13 Thickness loss for PNBHFANBC20 vs. development time in three different normality TMAH developers.

Two SEM images taken from the die that received 285 mJ/cm^2 exposure and developed for 15 seconds in 0.13 N TMAH are given in Fig. 4.14. The left one corresponds to the image taken by SEM tool with dim source beam and one on the right corresponds to the tool with bright source beam. The two images corresponding to the same die are shown side by side to emphasize the importance of the resolution capabilities of SEM tool that is being used. The resist material used was PNBHFANBC30. The right side SEM of Fig. 4.14 (brighter source beam) indicates that there is scumming observed at the line edges and the lines are actually 100 nm (instead of 150 nm). This condition is most probably due a combination of under development and over exposure. The scumming issue might be a result of the gel layer formation for PNBHFA in a

weak developer as mentioned in Hiroshi Ito's published papers. More optimization is required on development part in order to get the highest quality images possible from this system. The SEM image given in Fig. 4.15 corresponds to PNBHFANBC30 sample, but that time development time is extended to 45 seconds, followed by 15 sec water rinse. It indicates that extended development results in less scumming as predicted.

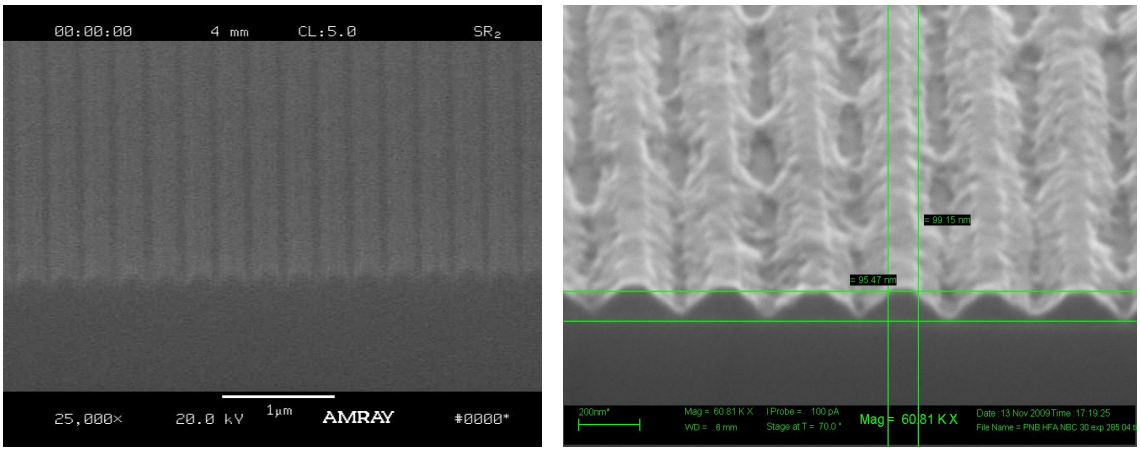

Figure 4.14 SEM images of 150 nm lines/spaces exposed at 285 mJ/cm^2 (PNBHFANBC30).

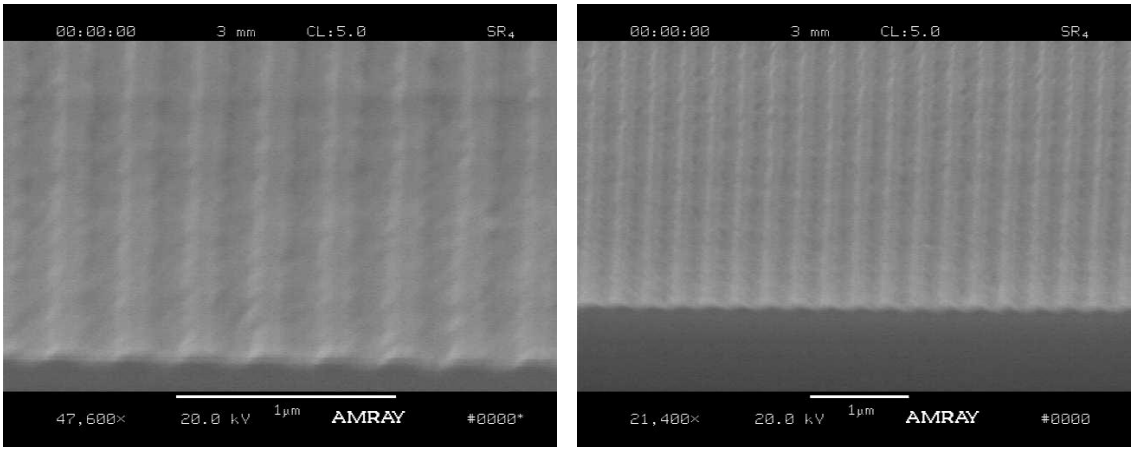

Figure 4.15 SEM images of 150 nm lines/spaces exposed at 249 mJ/cm^2 (PNBHFANBC30).

Several images are shown in Fig. 4.16 taken from different parts of a PNBHFANBC20 die that received 230 mJ/cm^2 exposure. The difference in these images for the same die might be due to local variation of developer strength and generated acid concentration upon exposure,

local endo/exo ratio, dose variation, etc. The development time was 45 seconds in 0.13 N TMAH, followed by 15 sec water rinse. Further study is essential for removing the residual layer and to better assess the resolution limit of this new two component resist system.

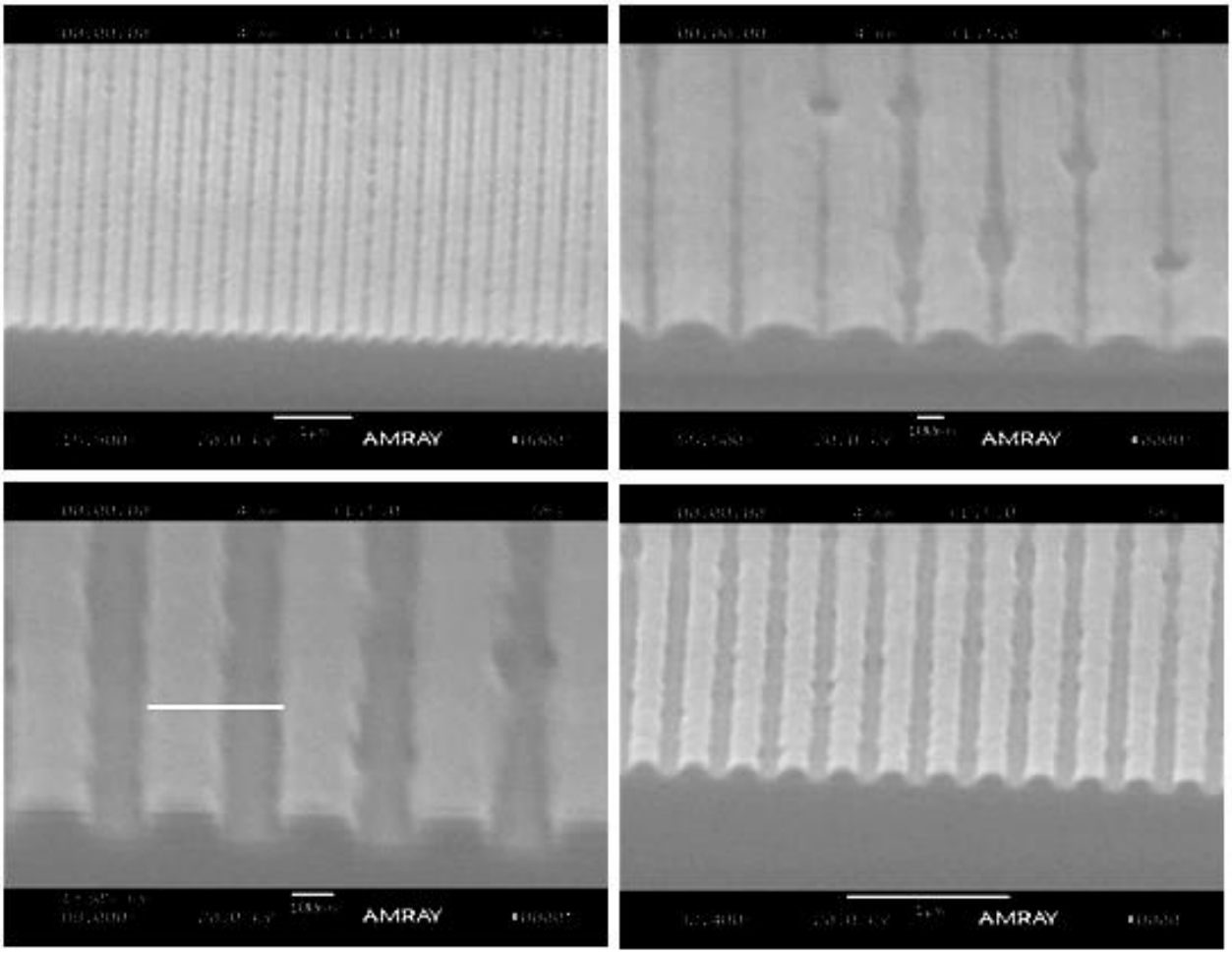

Figure 4.16 SEM images of 150 nm lines/spaces exposed at 230 mJ/cm^2 (PNBHFANBC20).

Fig. 4.17 shows 90 nm dense line/space pattern achieved by using PNBHFANBC30 . The developer used is 0.20 N TMAH and the development time is kept as 5 sec, followed by 30 sec water rinse. The resist thickness is 80 nm.

The imaging studies at 180 nm pitch are repeated for the (1:1) blend of PNBHFA and P(MMA/MAA) polymers blended with 30% NBC and the result is shown in Fig. 4.18. There is significant amount of roughness at the line edges and top surface.

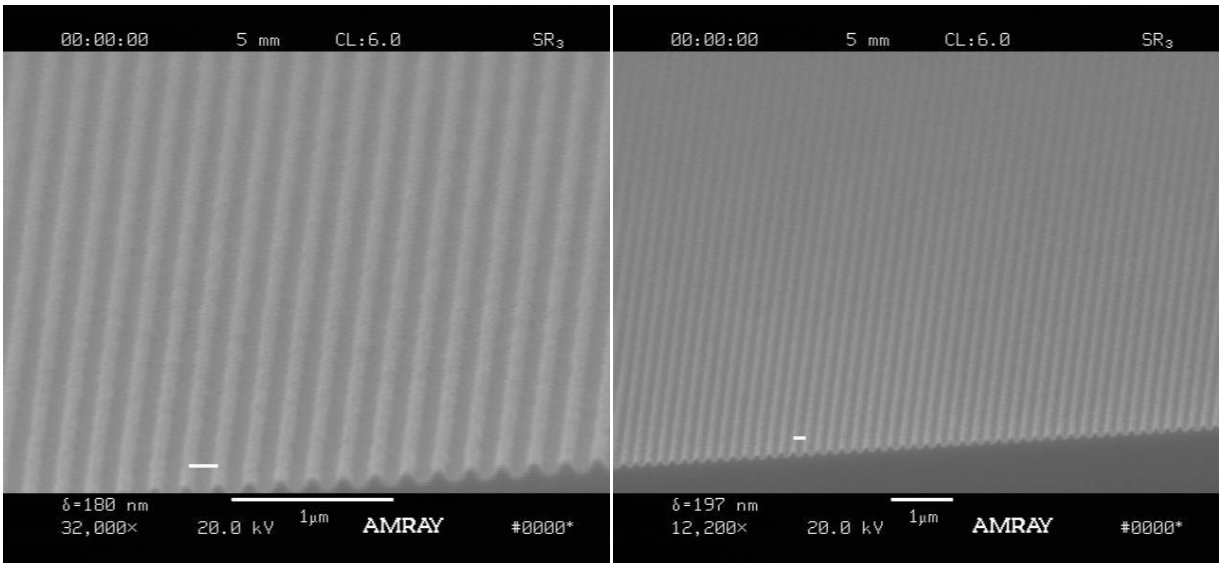

Figure 4.17 SEM images of 90 nm lines/spaces exposed at 300 mJ/cm^2 (PNBHFANBC30).

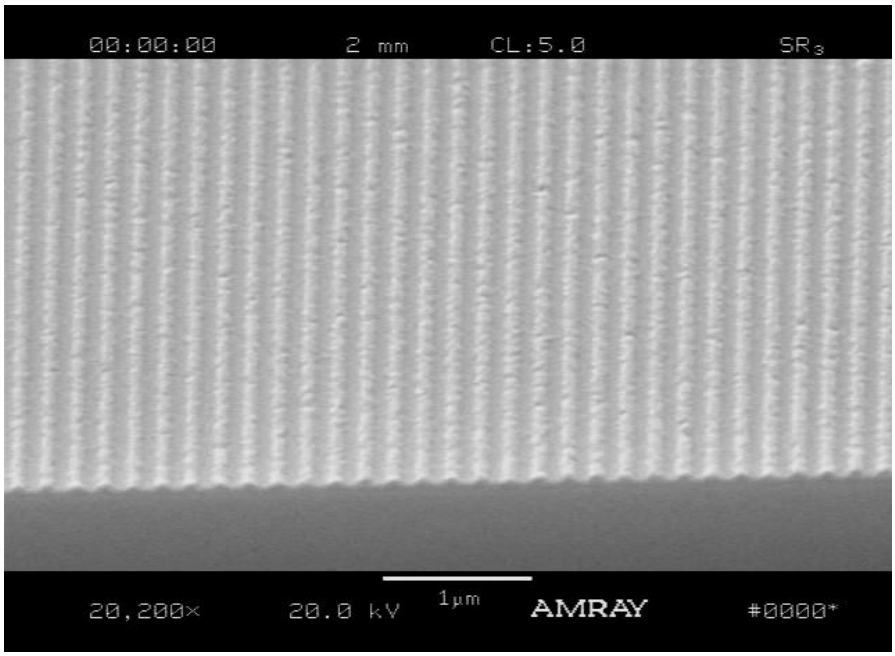

Figure 4.18 SEM images of 90 nm lines/spaces exposed at 300 mJ/cm^2. The resist is (1:1) blend of PNBHFA and P(MMA/MAA) loaded with 30% NBC.

Unfortunately, DNQ was found to be not miscible with PNBHFA and showed phase separation as shown in Fig. 4.19.

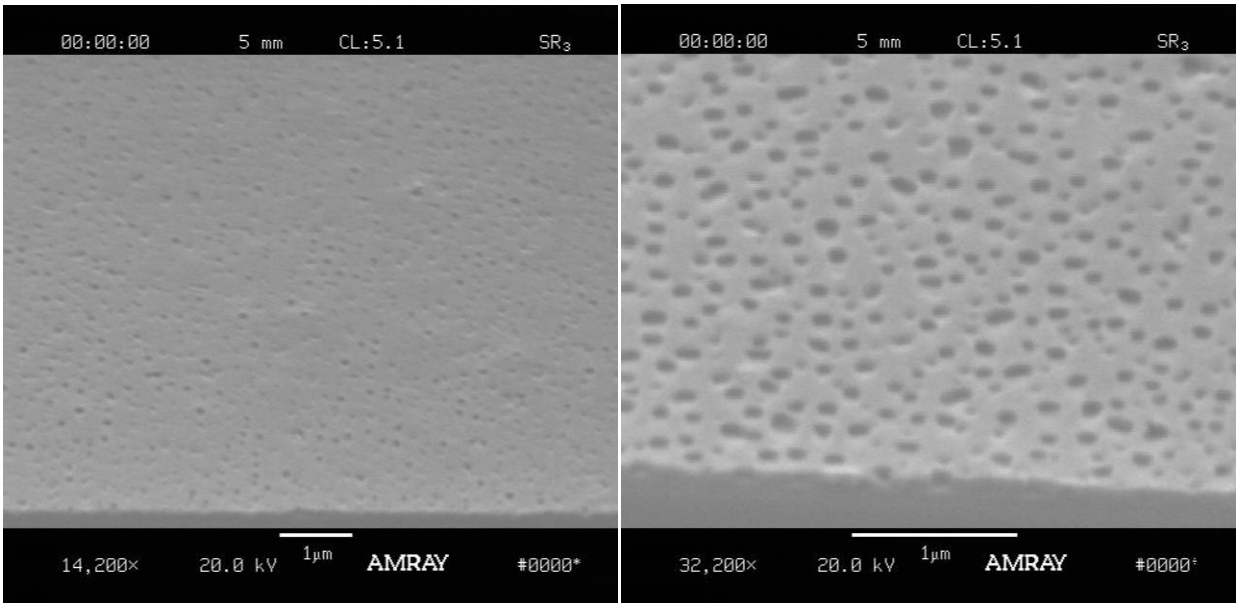

Figure 4.19 SEM images of the PNBHFA and DNQ blend (30% loading ratio) exposed at 300 mJ/cm^2 with ArF laser (PNBHFADNQ30). The pitch is again 180 nm.

4.3.4 Effect of Development Conditions on Imaging for PNBHFA System

Ito *et al.* reported specific dissolution kinetics for PNBHFA in a weak developer (like 0.21 N TMAH). One of the problems was gel layer formation (the semi dissolving layer in which acidic base resin reacted with alkaline ions from the developer). There is no such problem for a strong developer like 0.26 N TMAH which also shows almost linear dissolution rate. A development study is done in order to verify this and to clear semi dissolving layer at resist edges. BARC thickness is kept at 81 nm and the developer is again 0.13 N TMAH. PNBHFANBC20 film is exposed at 193 nm and the exposed die is developed for 30 sec followed by 30 sec water rinse, 45 sec followed by 45 sec water rinse and 60 sec followed by 60 sec rinse. The SEM images corresponding to three cases are shown in Fig. 4.20. The NA of exposure system is 0.39, corresponding to 120 nm lines/spaces. The conclusion from this study is

that the development conditions play a big role in imaging of PNBHHFA systems and blend of PNBHFA with NBC is capable of printing 120 nm dense patterns at 193 nm wavelength.

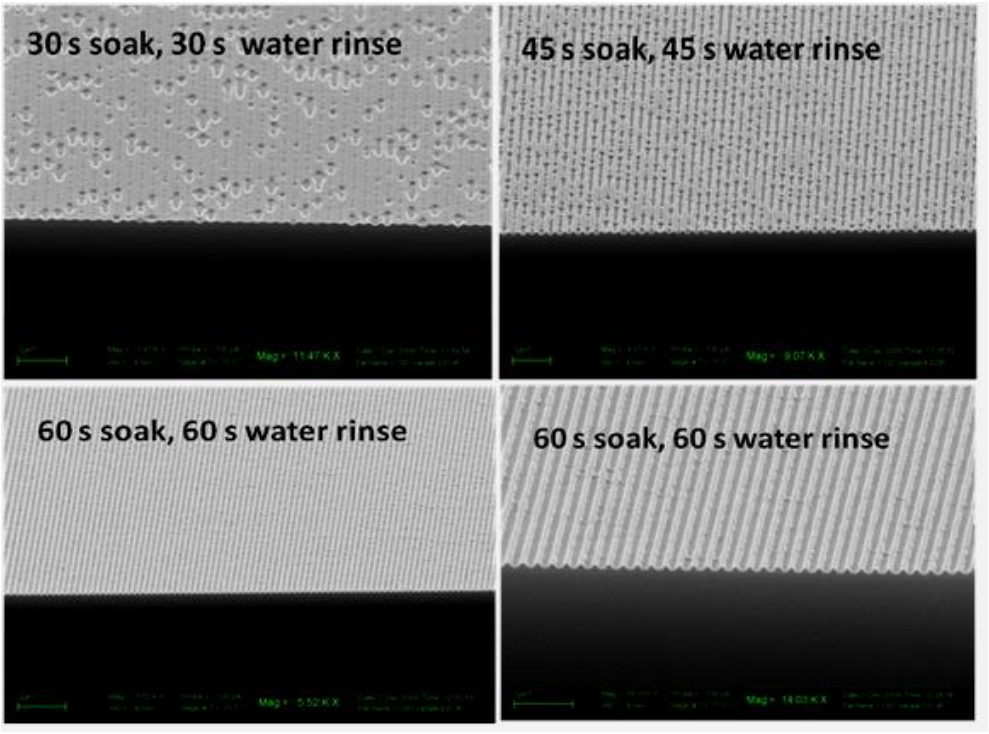

Figure 4.20 SEM images of 120 nm lines/spaces exposed with 193 nm laser showing effect of development conditions (PNBHFANBC20).

Chapter 5

Conclusions

The objective of this research was to come up with a two component, non-chemically amplified 193 nm photoresist system that is capable of high resolution at the expense of sensitivity. For this, three different base resins are examined: (i) P(MMA-co-MAA) copolymer, (ii) P(MA/NB/AA) terpolymer, and (iii) PNBHFA homopolymer. Among several options, *o*-nitrobenzyl cholate dissolution inhibitor was the primary choice to blend in resist matrix due to its low absorbance, miscibility in the base resin and high alicyclic carbon content.

The experiments showed that P(MMA-co-MAA) system is not capable of printing high resolution patterns. SEM images showed that resist side walls are not steep and the profiles look almost sinusoidal rather than squares.

The problem encountered with P(MA/NB/AA) was the inherent hydrostability issue and cracking, peeling, and non-uniform dissolution characteristics at the exposed regions. The polymer solution possessed limited shelf life and tendency to form di-acid moieties in existence of water.

Due to the problems observed for P(MMA-co-MAA) and P(NB/MA/AA), the experiments focused on PNBHFA homopolymer which was known to have good resolution, high plasma etch resistance and superior dissolution characteristics than carboxylic acid based photoresist materials.

The blends of PNBHFA with NBC was capable of printing 150 nm ,120 nm and 90 nm lines/spaces at 193 nm exposure and development conditions play a significant role in imaging.

SUMMARY

A two component system comprising alkaline soluble PNBHFA as the resin matrix and *o*-nitrobenzyl cholate (NBC) as the dissolution inhibitor is realized for the first time to be used for 193 nm lithography. The content of NBC can be as high as 30 % with respect to the polymer weight in the solution. 193 nm absorbance of 30 % NBC incorporated PNBHFA is less than 3 /μm which is suitable for very thin film lithographic applications. Both homopolymer and the NBC are known to possess high plasma etch resistance.

The developer for this system is strong alkaline solution. The strength of the developer and development condition (soak time/rinse time) are shown to affect the removal of residual layer attached to the pattern edges. The imaging capabilities of norbornene type polymer are shown to be superior to the acrylate type polymers.

REFERENCES

[1] ITRS. (2009, *International Technology Roadmap for Semiconductors 2007 Edition Lithography*. Available: http://www.itrs.net/reports.html

[2] Hinsberg W., Houle F., Sanchez M., Hoffnagle J., Wallraff G., Medeiros D., Gallatin G., Cobb J., *Proceedings of SPIE*, 5039, 2003

[3] Smith B. W., Yan F., Slocum M., Zavyalova L., *Proceedings of SPIE*, 5754, 2005

[4] Ueno T., Allen R., Chemistry of Photoresist Materials in Microlithography: Science and Technology, K. Suzuki and B. W. Smith, eds CRC Press, Taylor and Francis Group, Ch. 10&11, 2007

[5] Wallraff G., Medeiros D. R., Sanchez M., Petrillo K., Huan W. S., Rettner C., Davis B., *Journal of Vacum Science and Tech. B*, 22:3479, 2004

[6] Kaya S., Brown A. R., Asenov A., Magot D., Linton T., *Proc. SISPAD*, 2001

[7] Linton T., Chandhok M., Rice B. J., Schrom G., *IEDM Technical Digest*, 2002

[8] Gronheid R., Solak H. H., Ekinci Y., Jouve A., Roey F. V., *Microelectronic Engineering*, Vol. 83, pp. 1103-1106, 2006

[9] Rothschild M., Sedlacek J. H. C., *Proceedings of SPIE*, Vol. 1848, 537, 1992

[10] Kittelman O., Ringling J., *Opt. Lett. 19*, 2053 (1994)

[11] Rothschild M., Forte A. R., Kunz R. R., Palmateer S. C., Sedlacek J. H. C., *IBM J. Res. Dev.*, Volume 41, Numbers ½, 1997

[12] Komine N., Sakuma S., Shiozawa M., Mizugaki T., Sato E., *Applied Optics*, 39, pp. 3925-3930, 2000

[13] Mizuguchi M., Hosono H., Kawazoe H., Ogawa T., *J. Vac. Sci. Tech. A*, 16, pp. 3052-3057, 1998

[14] http://www.gigaphoton.com/technology/index.html

[15] Allen R. D., Wallraff G. M., Hinsberg W. D., Simpson L. L., *J. Vac. Sci Tech. B*, Vol. 9, pp. 3357-3361, 1991

[16] Allen R. D., Wallraff G. M., Hinsberg W. D., Conley W. E., Kunz R. R., Journal of Photopolymer Science and Technology, Vol. 6, No.4, pp.575-592, 1993

[17] Reichmanis E., C. W. Wilkins, Chandross E. A., *J. Vac. Sci. Technol.*, 19, 1338 (1981)

[18] Reichmanis E., C. W. Wilkins, Chandross E. A., *J. Electrochem. Soc.*, Volume 129, Issue 11, pp. 2552-2555 (1982)

[19] Reichmanis E., Gooden R., Wilkins C. W., Schonhorn H., *J. Poly. Sci., Poly. Chem. Ed. 21*, 1075-1083 (1983)

[20] Photosensitive Element Comprising a Substrate and an Alkaline Soluble Mixture, U.S. Patent 4,666,820, E. A. Chandross, E. Reichmanis, C. W. Wilkins

[21] Houlihan F. M., Wallow T., Timko A., Neria E., Hutton R., Cirelli R., Kometani J. M., Nalamasu O., Reichmanis E., Journal of Photopolymer Science and Technology, Vol. 10, Number 3, pp. 511-520, 1997

[22] H. Ito, N. Seehof, R. Sato, T. Nakayama, and M. Ueda, "Synthesis and evaluation of alicyclic backbone polymers for 193 nm lithography," *ACS Symposium Series 706, "Micro- and Nano-Patterning Polymers,"* H. Ito, E. Reichmanis, O. Nalamasu, and T. Ueno, Eds., American Chemical Society, Washington, D. C., Chap. 16, pp. 208- 223, 1998

[23] H. Ito, W. D. Hinsberg, L. F. Rhodes, C. Chang, "Hydrogen bonding and aqueous base dissolution behavior of hexafluoroisopropanol-bearing polymers," *Proceedings of SPIE,* Vol. 5039, pp.70-79, 2003

[24] H. Ito, H. D. Truong, L. F Rhodes, C. Chang, L. J. Langsdorf, H. A. Sideway, K. Maeda, S. Sumida, "Fluoropolymer Resists: Fundamentals and Lithographic Evaluation," *J. Photopolym. Sci. Technol.*, Vol. 17, No. 4, 2004

[25] C. R. Chambers, S. Kusumoto, G. Lee, A. Vasudev, L. Walthal, B. P. Osborn, P. Zimmerman, W. E. Conley, C. G. Wilson, "Dissolution inhibitors for 157 nm Photolithography," *Proceedings of SPIE,* Vol. 5039, pp. 93- 102, 2003

[26] Kiatkamjornwong S., Tessiri S., *Journal of Applied Polymer Science,* Vol. 86, pp. 1829–1837 (2002)

[27] Cortese F., Bauman L., *J. Biol. Chem.*, 113:779-785, 1936

[28] Jiang L., Chan T.-H., *J. Org. Chem.,* Vol. 63, pp. 6035-6038, 1998